

Award Number: W81XWH-11-1-0387

TITLE: Viral Oncolytic Therapeutics for Neoplastic Meningitis

PRINCIPAL INVESTIGATOR: Mikhail Papisov, PhD

CONTRACTING ORGANIZATION: Massachusetts General Hospital  
Boston, Massachusetts 02114

REPORT DATE: September 2014

TYPE OF REPORT: Final

PREPARED FOR: U.S. Army Medical Research and Materiel Command  
Fort Detrick, Maryland 21702-5012

DISTRIBUTION STATEMENT: Approved for Public Release;  
Distribution Unlimited

The views, opinions and/or findings contained in this report are those of the author(s) and should not be construed as an official Department of the Army position, policy or decision unless so designated by other documentation.

REPORT DOCUMENTATION PAGE				Form Approved OMB No. 0704-0188	
Public reporting burden for this collection of information is estimated to average 1 hour per response, including the time for reviewing instructions, searching existing data sources, gathering and maintaining the data needed, and completing and reviewing this collection of information. Send comments regarding this burden estimate or any other aspect of this collection of information, including suggestions for reducing this burden to Department of Defense, Washington Headquarters Services, Directorate for Information Operations and Reports (0704-0188), 1215 Jefferson Davis Highway, Suite 1204, Arlington, VA 22202-4302. Respondents should be aware that notwithstanding any other provision of law, no person shall be subject to any penalty for failing to comply with a collection of information if it does not display a currently valid OMB control number. <b>PLEASE DO NOT RETURN YOUR FORM TO THE ABOVE ADDRESS.</b>					
1. REPORT DATE September 2014		2. REPORT TYPE Final		3. DATES COVERED 1 July 2011 – 30 June 2014	
4. TITLE AND SUBTITLE Viral Oncolytic Therapeutics for Neoplastic Meningitis				5a. CONTRACT NUMBER	
				5b. GRANT NUMBER W81XWH-11-1-0387	
				5c. PROGRAM ELEMENT NUMBER	
6. AUTHOR(S) M. Papisov  E-Mail: Papisov@helix.mgh.harvard.edu				5d. PROJECT NUMBER	
				5e. TASK NUMBER	
				5f. WORK UNIT NUMBER	
7. PERFORMING ORGANIZATION NAME(S) AND ADDRESS(ES)  Massachusetts General Hospital Boston, Massachusetts 02114				8. PERFORMING ORGANIZATION REPORT NUMBER	
9. SPONSORING / MONITORING AGENCY NAME(S) AND ADDRESS(ES) U.S. Army Medical Research and Materiel Command Fort Detrick, Maryland 21702-5012				10. SPONSOR/MONITOR'S ACRONYM(S)	
				11. SPONSOR/MONITOR'S REPORT NUMBER(S)	
12. DISTRIBUTION / AVAILABILITY STATEMENT Approved for Public Release; Distribution Unlimited					
13. SUPPLEMENTARY NOTES					
14. ABSTRACT  The goal of this collaborative exploratory project is to develop novel, safe and efficient therapy for neoplastic meningitis (meningeal metastasis of breast cancer). The proposed therapy will be based on direct (intrathecal) administration of oncolytic viruses into the cerebrospinal fluid (CSF). During the first research year, physiology of the intrathecal delivery of particles was studied in rats. The data was compared with the results obtained in non-human primates in our parallel studies. The key findings are the following. (1) The key factor defining the patterns of the initial particle distribution between the cerebral and spinal CSF is the volume of the bolus. (2) The key physiological factors defining further transport of the particles in the leptomeningeal space (and further into perivascular spaces) are tissue pulsation and particle interaction with the arachnoid. The data of the functional investigation of the diameter of meningeal pores draining CSF to the systemic circulation suggests a new, previously unreported subset of leptomeningeal pores that require further investigation. The new mechanistic model of particle transport in the leptomeningeal space supports the initial idea of the study and suggests further development of therapies for neoplastic meningitis based on oncolytic viruses.					
15. SUBJECT TERMS Neoplastic meningitis, leptomeningeal space, viral oncolysis, cerebrospinal fluid, drug delivery					
16. SECURITY CLASSIFICATION OF:			17. LIMITATION OF ABSTRACT	18. NUMBER OF PAGES	19a. NAME OF RESPONSIBLE PERSON
a. REPORT Unclassified	b. ABSTRACT Unclassified	c. THIS PAGE Unclassified			USAMRMC
			Unclassified	48	19b. TELEPHONE NUMBER (include area code)

## Table of Contents

	<u>Page</u>
Introduction.....	4
Keywords.....	5
Overall Project Summary.....	6
Key Research Accomplishments.....	12
Conclusions.....	13
Reportable Outcomes.....	14
Other Achievements.....	16
References.....	18
Personnel.....	18
Appendices.....	19

## INTRODUCTION

The overall goal of our studies is to develop novel, safe and efficient therapy for neoplastic meningitis.

Neoplastic meningitis is a devastating complication of breast cancer caused by the spread of breast cancer cells into layers of tissues surrounding the brain that are normally filled with fluid. The space between two layers of isolating tissues enveloping the brain where neoplastic meningitis develops is isolated from the rest of the body and is not accessible to drug molecules circulating in blood.

This exploratory “Idea” project was aimed at the development of a drug of a novel type that would not escape from the space where the cancer cells spread causing neoplastic meningitis. We proposed that an engineered virus hrR3, capable of killing cancer cells but harmless for normal tissues, will stay between the isolating tissue layers where the cancer cells spread, and kill them much more effectively than conventional drugs.

The objectives of this exploratory study were to determine whether the hrR3 suspensions can stay in the area surrounding the brain for a period of time sufficient to infect the meningeal cancer cells, to evaluate the safety, and to estimate the most effective schedule of hrR3 administration.

The study was carried out generally as planned. The outcome of the study is threefold:

- (1) The data confirms the original idea that the pharmacokinetics of engineered viruses can enable virus access to the meningeal cancer cells.
- (2) The data show that the existing paradigm of intrathecal drug delivery is based on incomplete experimental evidence and includes multiple misinterpretations of the mechanistic factors, directionality and timing of solute transport in the CSF. The potential value of intrathecal drug delivery to meningeal targets as well as to CNS is significantly larger than presently believed (but requires developing drugs specifically optimized for this delivery route)
- (3) The previously developed rodent models of neoplastic meningitis and intrathecal drug administration are not suitable for routine investigation of intrathecal treatment of meningeal cancer and need further development.

## **KEYWORDS**

Neoplastic meningitis, Cerebrospinal fluid, Meninges, Cancer, Positron Emission Tomography, Intrathecal

## OVERAL PROJECT SUMMARY

The project was structured as follows:

**Aim 1.** To fully characterize hrR3 as intrathecal pharmaceutical.

- 1.1. Characterize the viral suspension obtained in cell cultures (particle size distribution, aggregation); develop a method for isolation of highly fractionated monomers and oligomers.
- 1.2. Investigate the dependence of the retention of radiolabeled virions (single particles and oligomers) in CSF (PET imaging). Select the optimal particle size.

**Aim 2.** To evaluate the efficacy and safety of viral suspensions in an animal model of meningeal cancer spread.

- 2.1. Determine the maximum tolerated intrathecal dose (MTD) of the virus.
- 2.2. Investigate the dynamics of viral expression in the leptomeningeal cancer by PET.
- 2.3. Investigate the efficacy of the virus in a meningeal cancer spread model.

Tasks of Aim 1 were carried out during the first year of research (2012). Due to major renovations of the BSL-2 compliant animal facilities compatible with the use of radionuclides, as needed for this study, the tasks of Aim 2 were delayed and carried out through the third (extended) year of research (2014).

Studies of Aim 1 (the previous funded period, 2011-2013) have shown that:

- (a) Viral suspensions (provided by Dr. Kuruppu, co-PI on this two-PI project) consisted mostly of mono-virions and did not require fractionation.
- (b) The initial particle distribution in the CSF depends on the volume of the intrathecal bolus. The larger the volume of a lumbar bolus, the larger fraction of the dose is translocated towards cerebral CSF.
- (c) In rats and monkeys the CSF is remixed by tissue pulsation. The rate of remixing enables solute translocation from the lumbar site to cisterna magna within about 5 hours in both rats and monkeys. Hydrophobic particles are not transported with the CSF, presumably due to non-specific binding to the arachnoid. Virions behave generally as hydrophilic particles and can be transported across the CSF sub-compartments. It was noticed, however, that a variable fraction of the administered dose of hrR3 was deposited in the near vicinity of the catheter/needle tip.
- (d) In addition to the well described large (1-8 microns) meningeal pores in the arachnoid granulations, there is at least one smaller, previously uncharacterized

subset of pores (location unknown). Published in Proceedings papers [4] and Abstracts [7-11].

Overall, the results of the studies conducted during the first year suggested a new mechanistic model of particle transport in the leptomeningeal space, which strongly supported the feasibility of the initial idea of the study and suggests further development in accordance with the original plan.

The experimental methods, data and analysis of the above observations have been published (Full size research papers [1] and [2], respectively).

The new mechanistic understanding of the physiology of cerebrospinal transport suggested farther investigation of the pharmacokinetic factors that have never been discussed in the literature but were crucial for understanding and modeling of the virion transport in the CSF, the patterns of which were critically important for all Tasks of the funded period (2014). Therefore, each respective Task was supplemented with experiments necessary for mechanistic interpretation of the data, as follows.

Studies of Aim 2 (year 2, extended to year 3: 2013-2014).

**Task:** Determine intrathecal MTD of hrR3 (Aim 2.1). The MTD was first investigated in mice in a dose elevation experiment, as planned. At  $10^9$  pfu/kg (10X expected therapeutic dose) MTD was not reached. Then, in view of the potential differences in the virion distribution in rats and mice, the result was verified in nude rats. At  $10^9$  pfu/kg MTD was not reached as well (not yet published).

**Task:** PET imaging and photoimaging studies of viral expression (Aim 2.2) - see the co-PI's Annual report.

**Task:** Investigate the efficacy of the virus in a meningeal cancer spread model, single and multiple injection studies (Aim 2.3).

Since it was noticed during the year 1 studies in rats that after intrathecal injection a variable fraction of the administered dose of hrR3 was deposited in the near vicinity of the catheter/needle tip, it was important to determine the cause of the deposition as well as its variability. Our previous studies on enzyme transport in the CSF in monkeys (*M. fascicularis*) after lumbar intrathecal and intracerebroventricular administration showed much lower variability of the agent deposition than in rats. Therefore we decided to investigate hrR3 transport in this species (Scheme of experiment: Figure 1). We carried out two real-time PET studies of hrR3 transport in the CSF of monkeys with  $^{89}\text{Zr}$ -labeled hrR3. We have found that radiolabeling with  $^{89}\text{Zr}$  gives better results in Positron Emission Tomography (PET) than the originally planned radioiodination with  $^{124}\text{I}$  (published in Abstracts [12]).

Scheme of the experiment is shown in Figure 1.

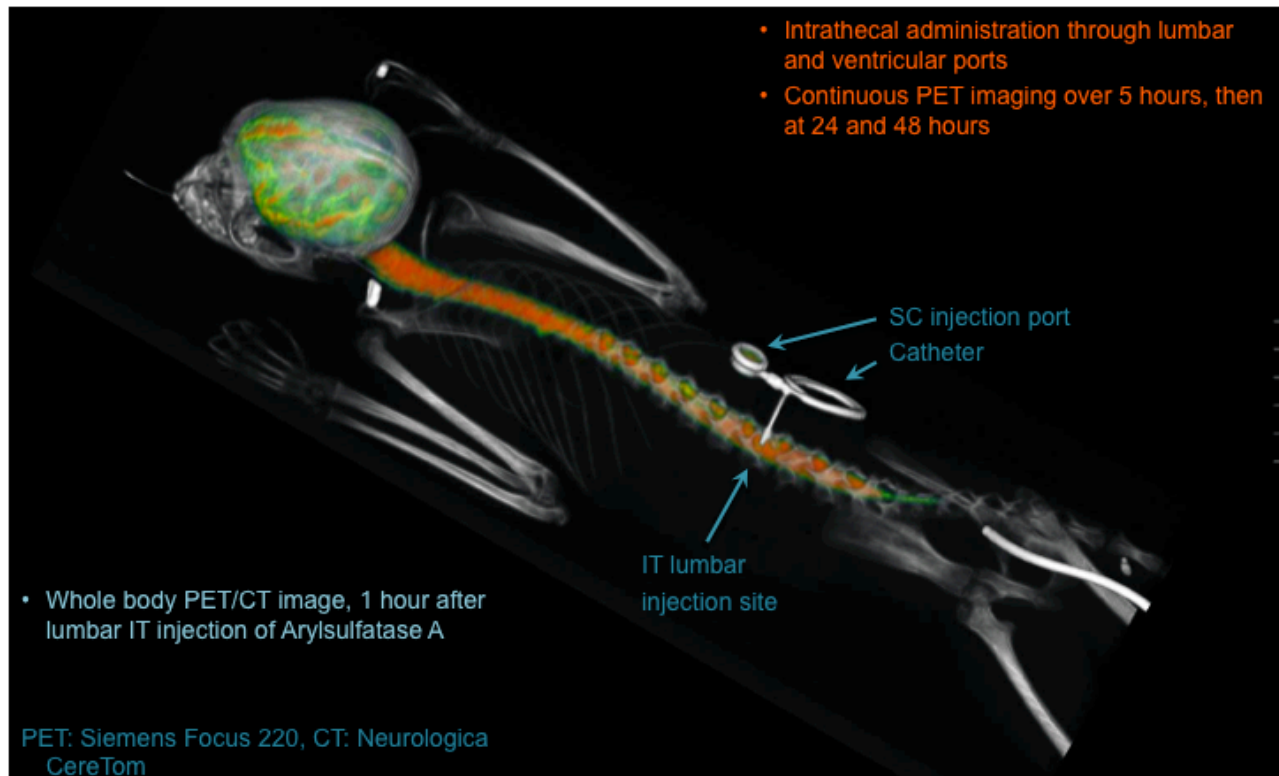


Figure 1. Scheme of experiment in *M. Fascicularis* (PET/CT image acquired earlier in studies on enzyme transport in the CSF). The radiolabeled test substance was administered through the pre-installed SC injection port opening into the CSF. Whole body PET/CT images were acquired 0.5 hours after the injection and at later time points. The amount of radioactivity in each 1 mm transversal slice was determined; the distribution graphs are shown in Figure 2. Methods published in Proceedings papers [3] and [5].

The data (Figure 2) have shown that: (a) the virions can be delivered from the lumbar catheter opening at L1-L2 throughout the entire CSF compartment via one large-volume lumbar intrathecal bolus, and (b) the virions, unlike model nanoparticles and proteins, lose their mobility in the CSF and are not transferred to the systemic circulation (>95% retention in the leptomeningeal space).

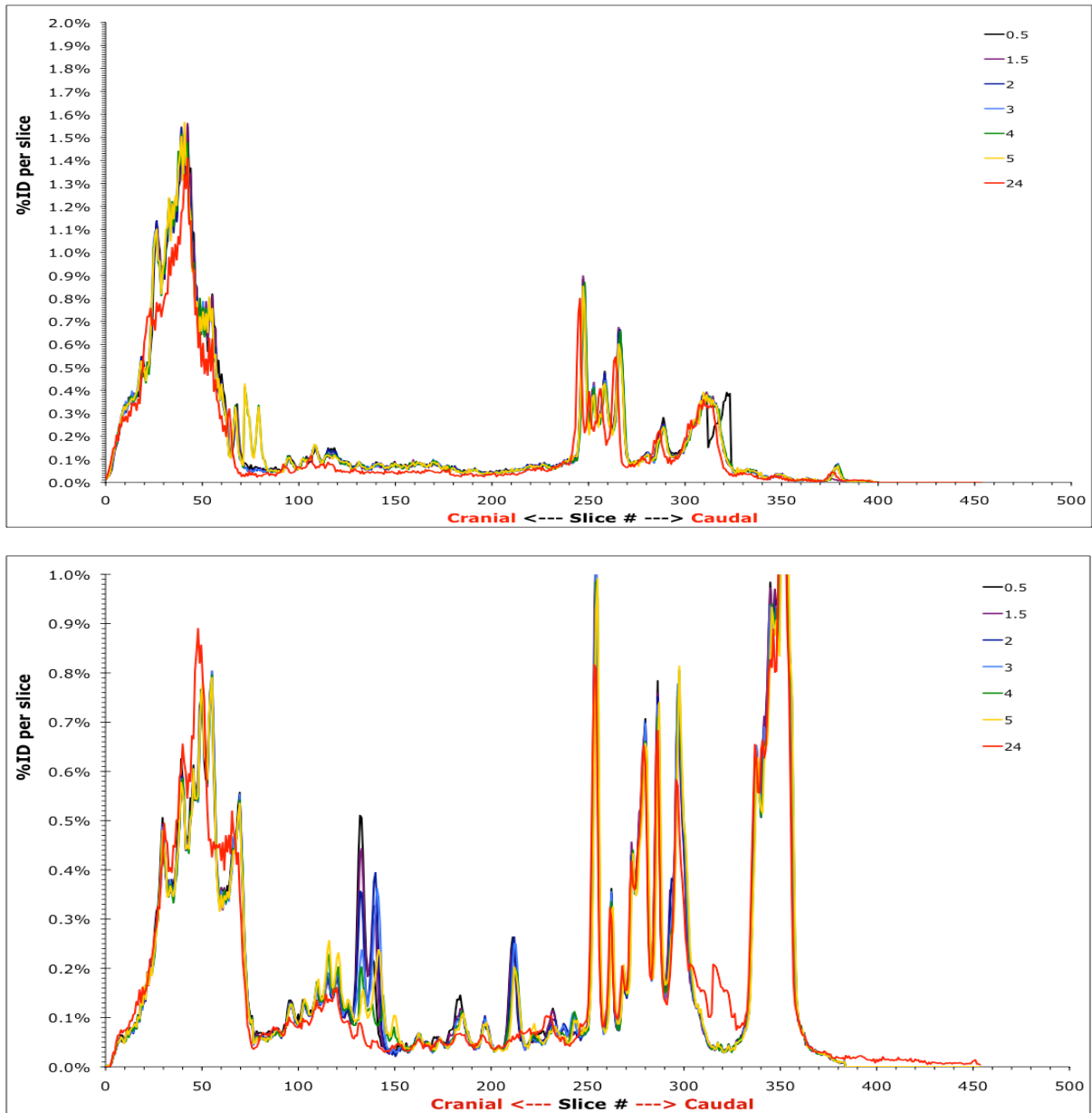


Figure 2. The dynamics of hrR3 in the CSF of *M. fascicularis*. Distribution of radioactivity per 1 mm slice across subarachnoid space at 0.5 to 24 hours after lumbar intrathecal injection (scheme of experiment in Figure 2). Two animals. Animal heads are at the left.

Note: (A) significant initial deposition of the administered material in the injection port area and (B) negligible clearance over 24 hours.

Typical data for an analogously administered enzyme with no deposition near the port and significant clearance from the CSF is given for comparison in Figure 3.

Pertially published in Proceedings papers [6] and Abstracts [13]; full size manuscript is in preparation.

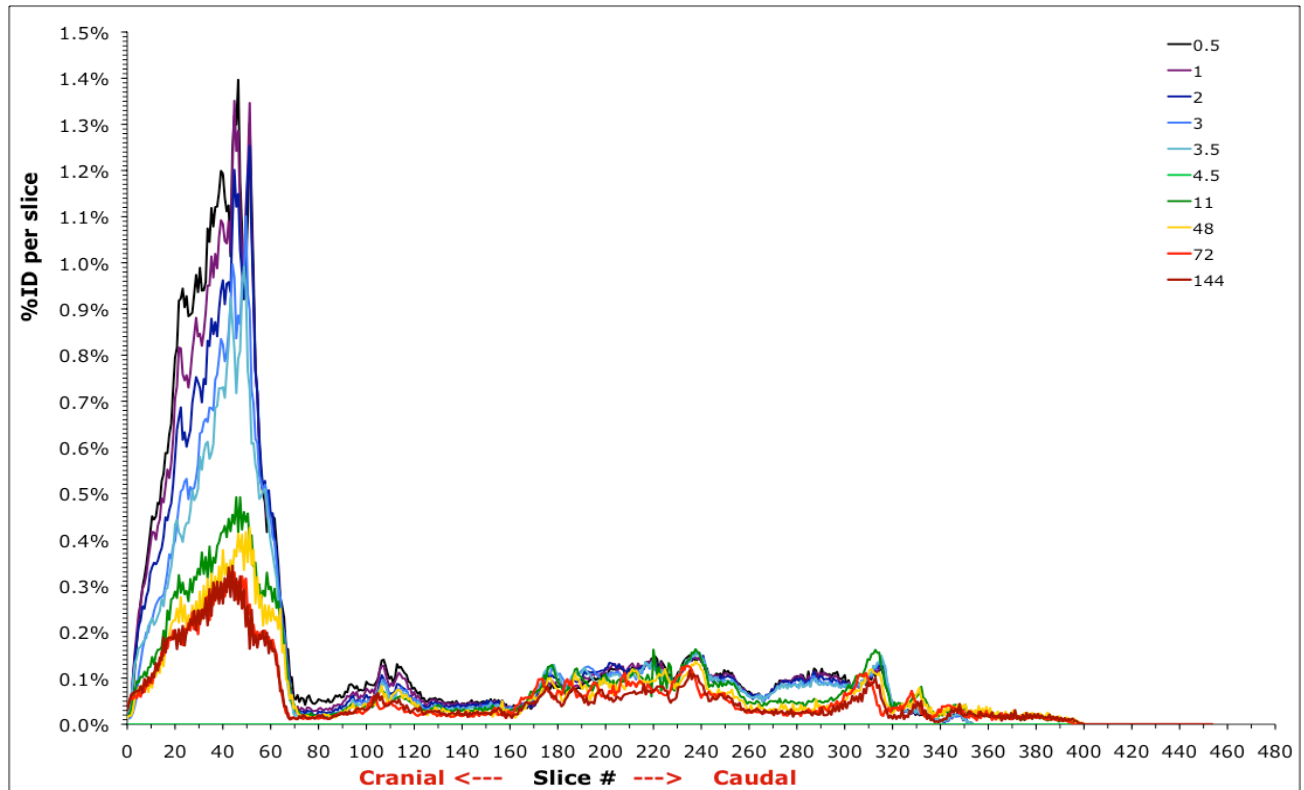


Figure 3. (Not yet published) The dynamics of an enzyme (NAGlu) in the CSF of *M. fascicularis*. Distribution of radioactivity per 1 mm slice across subarachnoid space at 0.5 to 144 hours after lumbar intrathecal injection. Animal head is at the left (the same animal as in Figure 2, top).

Note: (A) No initial deposition of the administered material in the injection port area and (B) significant clearance over 24 hours.

The data obtained in monkeys suggest that hrR3 virions can rapidly (within minutes) bind the arachnoid, which precludes their redistribution in the CSF after the initial hydrostatic compliance-dependent translocation as well as clearance from the subarachnoid space to the systemic circulation. The latter was also confirmed by very low virion accumulation in the liver and spleen (not shown).

The data was partially published (Proceeding papers [6]); full manuscript is in preparation.

On one hand, this virion binding to the arachnoid is a positive feature of hrR3 pharmacokinetics that prevents fast clearance of the potential therapeutic from the CSF.

On the other hand, rapid hrR3 binding to normal arachnoid component suggests that a

significant fraction of the dose will bind non-target cells and the virions may not have enough time to penetrate deep into the perivascular spaces (which is a slow process that requires particle presence in the liquid CSF phase for several hours). Thus, the data suggest that delivery of unmodified virions to the cerebrospinal fluid may not guarantee virus access to cancer cells spreading into the perivascular spaces. Therefore, the virions may need to be modified to reduce their affinity to normal arachnoid. Development of such virions will be one of the objectives of the future studies.

The need to deliver hrR3 in one fast bolus for significant coverage of the subarachnoid space suggests further optimization of the rodent models used in meningeal cancer research. The data suggest that the patterns of delivery of cancer cells to the subarachnoid space may also depend on the bolus volume and injection rate. Thus, experimental evaluation of the distribution of cancer cells after intrathecal administration as a function of injection volume and rate is warranted.

Studies of Aim 2 have shown that intrathecal administration of hrR3 in rodents is well tolerated. The dynamics of cancer spread was investigated in mice by the co-PI's group as our studies with cannulated nude rats showed (in quality control experiments with injection monitoring by PET) multiple problems with this animal model beyond the uncertain cell distribution described above. Based on our previous experience with outbred rats, direct non-surgical injection into cisterna magna through the atlanto-occipital joint was planned as the method of implantation. We have found in pilot experiments with Rnu/nu rats that the configuration of the atlanto-occipital region in this strain is somewhat different, and the direct injection (which would enable fast administration of relatively large volumes) results in a higher frequency of experimental failure, ca. 40% vs. 20% for CD rats as performed by the same personnel.

To develop an alternative cell infusion method, we worked with our animal vendor, Charles River Laboratories (CRL), to adopt their intrathecal catheterization service for this purpose. Cannulated animals from CRL were administered with model radiolabeled particles through the catheters, and the particulate distribution was studied by PET. It was found that the conventional lumbar cannulation with caudad catheter tip placement resulted in frequent (~ 50%) blockage of particle passage towards the cerebral CSF volume, which is not acceptable for meningeal cancer studies. On our request, CRL changed the direction of the catheter tip placement to the anteriad. With anteriorly oriented catheters, particle passage towards the cranium was observed in about 80% of the animals. This can be considered satisfactory, provided that (a) every injection is monitored for quality by PET and (b) the catheter lumen is wide enough to deliver cell and viral suspensions as relatively fast (<1 min) large volume (>30 ml) bolus. Also, the catheter patency was found to be shorter than a week, which precluded the use of these (polyolefine) catheters for studies where cancer cell and virion administrations should be carried out over an at least two week period (cancer cell infusion and then oncolytic virus administration). Thus, development of long-leaving (>20 days) catheters leading to cisterna magna is necessary for studies on intrathecal therapy of meningeal cancer and may require catheter impregnation with a controlled amount of a cytostatic material (which warrants a separate product-oriented study). Development of new protocols was

unfortunately beyond the timeframe and budget of this pilot “idea” study.

Thus, both experimental approaches, catheterization did not allow us to obtain statistically significant therapeutic efficacy data in the small groups of animals planned for this exploratory project. However, the project resulted in new mechanistic quantitative data on the physiology of solute transport in the cerebrospinal fluid that differed from the current paradigm of cerebrospinal transport beyond all expectations. The new mechanistic paradigm of solute transport in the CSF opens valuable new opportunities for drug delivery to meningeal and CNS targets (to meningeal cancer in particular) and provide very clear guidance for the future research on developing intrathecal therapies for neoplastic meningitis.

### **KEY RESEARCH ACCOMPLISHMENTS:**

- A new mechanistic paradigm of solute transport in the leptomeningeal space developed. The mechanisms of solute transport include a hydrostatically controlled early stage, where the hydrostatic compliance of the compartment directs a large volume (>10% of the total CSF volume) bolus towards the cervical CSF pool. The compliant anatomical elements are not yet known. The subsequent hydrodynamically controlled transport in the cerebral and cervical CSF is non-directional and unexpectedly fast (full remixing in ~ 20 minutes in both rodents and monkeys), whereas solute transport in the spinal CSF is also non-directional but slow (single millimeters per hour). The rates and directionality of transport are consistent with biomechanical CSF remixing by pulsatile movements of arteries and CNS tissues.
- A previously uncharacterized subset of meningeal pores (or processes functionally analogous to pores) leading from the CSF to the systemic circulation is demonstrated. Pore diameter is <20 nm (in contrast to the known > 1 µm pores in the arachnoid granulations)
- A mechanistic basis for scalability of the intrathecal bolus pharmacokinetics from the rodent model to larger animals and humans is established, based on the timing of the hydrostatically and hydrodynamically controlled stages of the intrathecal bolus.
- Well defined objectives for the future studies on the therapy of neoplastic meningitis with hrR3: optimization of the rodent models and targeted surface modification of the virion to maximize the bioavailability (target-to-normal tissue ratio).

The data obtained in this study points at the necessity to further investigate the mechanisms of solute transport in the CSF and from the CSF to the perivascular space.

The results obtained in the study enabled us to obtain funding for investigation of these factors: NIH 1R01NS092838-01, “Factors of cerebrospinal drug transport”, and NIH

1R21NS090049-01, “Investigation of solute transport from the cerebrospinal fluid to CNS”. The results of these ongoing studies will enable further rational development of oncolytic therapeutics optimized for intrathecal treatment of neoplastic meningitis.

## **CONCLUSIONS:**

The research completed to date supports the feasibility of the original idea of this exploratory project.

The cerebrospinal transport of virions depends on the hydrostatic factors driving the administered volume to the cervical CSF, hydrodynamic factors remixing the CSF, size-dependent particle clearance from the CSF, and virion interaction with normal arachnoid components. The interplay of these factors defines the bioavailability and needs further investigation.

The new physiological data further suggest that complete coverage of the leptomeningeal space with intrathecally administered oncolytic viral suspensions is possible, preferably with a large volume bolus and likely with modified (for optimal arachnoid binding) virions. Further studies in this direction are warranted and should include animal model refinement with catheter patency optimization and monitoring (e.g. by PET).

More broadly, the mechanistic physiological data obtained in this study, in combination with other studies on cerebrospinal drug transport conducted in our laboratory, strongly suggest that intrathecal drug administration has been underutilized.

## **REPORTABLE OUTCOMES:**

### **Full size research papers:**

1. Papisov M, Belov V, Fischman A.J., Belova E, Titus J, Gagne M., Gillooly C. Delivery of proteins to CNS as seen and measured by Positron Emission Tomography. Drug Delivery and Translational Research 2012, 2:201-209
2. Papisov M, Belov VV and Gannon KS. Physiology of the intrathecal bolus: the leptomeningeal route for macromolecule and particle delivery to CNS. Molecular Pharmaceutics 2013, 10:1522-1532, DOI: 10.1021/mp300474m

### **Proceedings papers:**

3. M. Papisov, V. Belov, A.J. Fischman, J. Titus, M. Gagne, P. Calias, T. McCauley, M. Heartlein. Delivery of enzyme replacement therapeutics to CNS in rats and monkeys as seen and measured by PET. 39th Annual Meeting of the Controlled Release Society, Quebec, Canada, July 2012
4. Belova E, Vallance L, Belov V, Gagne M, Gillooly C, Papisov MI. PET-based approaches to studying the size-dependence of leptomeningeal drug clearance. 39th Annual Meeting of the Controlled Release Society, Quebec, Canada, July 2012.
5. Belov V, Papisov M. A PET based method for real time monitoring of drug concentration in the liquid phase of the leptomeningeal compartment. 39th Annual Meeting of the Controlled Release Society, Quebec, Canada, July 2012.
6. Papisov M.I., Belov V., Fischman A.J., Titus J., Gagne M., Gillooly C., Bonab A., and Levine D. Physiology of intrathecal bolus as revealed by quantitative PET studies. 41st Annual Meeting of the Controlled Release Society, Chicago, IL, July 2014.

### **Abstracts:**

7. Papisov M, Belov V, Fischman A, Titus J, Gillooly C, Gagne M. PET imaging of macromolecule and particle delivery to the brain through intrathecal administration in rodents and non-human primates. 2012 SNM Annual Meeting, Miami, FL.

8. Belov V, Fischman A, Bonab A, Papisov M. Assessment of the prompt !-coincidences background from the I-124 activity inside and outside FOV. 2012 SNM Annual Meeting, Miami, FL.
9. Belova E, V. Belov V, Gagne M, Gillooly C, Fischman AJ, Papisov MI. Pharmacokinetics of macromolecules in spinal CSF: PET and modeling. 2013 SNM Annual Meeting, Vancouver, BC, Canada.
10. Gillooly C, V. Belov V, Belova E, Gagne M, Fischman AJ, Titus J, Papisov MI. Assessment of CSF drainage to the lymphatic system using positron emission tomography in rats and nonhuman primates. 2013 SNM Annual Meeting, Vancouver, BC, Canada.
11. Bonab A, Fischman AJ, Belov V, Papisov MI. Biokinetics of FDG after intrathecal administration. 2013 SNM Annual Meeting, Vancouver, BC, Canada.
12. V. Belov, D. Levine, E. Belova, C. Gillooly, C. Mushti, M. Gagne, A.A. Bonab, A.J. Fischman, and M. Papisov. Pharmacological PET imaging performance with I-124 and Zr-89. 2014 SNM Annual Meeting, St. Louis, MO.
13. Papisov M, Belov V, Fischman AJ, Bonab A, Levine D, and Shi R. The dynamics of intrathecal bolus and cerebrospinal solute transport. SNM Annual Meeting, Baltimore, MD, June 2015.

#### **Inventions, Patents and Licenses:**

None filed. However, it is expected that the data of this study, in combination with presently performed internally funded follow-up studies, will lead to at least one patent application (of which DoD will be informed when/if filed).

## OTHER ACHIEVEMENTS

### Awards:

1. Outstanding Pharmaceutical Paper Award. Controlled Release Society, 2012.  
<http://www.controlledreleasesociety.org/about/Awards/Pages/OutstandingPharmaceuticalPaper.aspx>,  
<http://www.controlledreleasesociety.org/publications/Newsletter/Documents/v29i4.pdf>

### Degrees obtained:

2. Lloyd Vallance, MLA (Biotechnology), Harvard Extension School, 2012.

### Grant applications based on the results of this study:

#### AWARDED

- |                                   |   |
|-----------------------------------|---|
| 2. PI Papisov NIH 1R01NS092838-01 | Factors of cerebrospinal drug transport. <i>This study is intended to investigate the hydrostatic and hydrodynamic factors regulating transport processes in the cerebrospinal fluid, which will help developing new approaches for delivery of therapies, in particular biopharmaceuticals, to the central nervous system and meninges. This will provide novel effective therapies for diseases involving these tissues, such as, Parkinson's and Alzheimer's diseases, inherited genetic deficiencies, brain cancer and neoplastic meningitis. 2015-2018</i> |
| 1. PI Papisov NIH 1R21NS090049-01 | Investigation of solute transport from the cerebrospinal fluid to CNS. <i>The goal is to investigate solute transport from the CSF to the CNS parenchyma through perivascular conduits. 2014-2016</i>   |
| 3. PI: Belov MGH ECOR grant       | "Size dependent mechanisms of drug clearance from the cerebrospinal fluid". 2015.   |

PENDING

1. PI: Belov R21 grant application "Size dependent mechanisms of drug clearance from the cerebrospinal fluid", NIH, 2014, (Under review)

### **Invited lectures:**

1. "Macromolecular drug development and the role of PET imaging." Northeastern University School of Pharmacy, Department of Pharmaceutical Sciences Colloquium, 2012
2. "CSF solute dynamics as seen by PET", 2nd International Cerebrospinal fluid Dynamics Dynamics, Manhasset, NY. Sponsor: Chiari and Syringomyelia Foundation, 2013
3. "Pharmacological PET Imaging". Voyager Pharmaceutical, Cambridge, MA, 2014
4. "Cerebrospinal fluid dynamics: solute transport as seen by positron emission tomography". 7th World Congress of Biomechanics, Boston, 2014
5. "Solute transport in the CSF". 3rd International Cerebrospinal fluid Dynamics Dynamics, Amiens, France, 2015
6. "PET Imaging of solute transport in the CSF" New York University, 2015

### **Career development:**

Two BS-level participants, Matthew Gagne and Caitlin Gillooly, were accepted to a PhD program and Medical School, respectively.

The PI, M. Papisov, has been accepted as full member of Dana Farber/Harvard Cancer Center (Breast Cancer, Neuro-Oncology)

## **REFERENCES**

- See list of publications in the “Reportable Outcomes” above.

## **PERSONNEL**

Mikhail Papisov, PhD (PI)

Vasily Belov, PhD

Matthew Gagne, BS

Caitlin Gillooly, BS

James Titus, BS

## **APPENDICES:**

### **Full size research papers:**

Papisov M, Belov V, Fischman A.J., Belova E, Titus J, Gagne M., Gillooly C. Delivery of proteins to CNS as seen and measured by Positron Emission Tomography. Drug Delivery and Translational Research 2012, 2:201-209

Papisov M, Belov VV and Gannon KS. Physiology of the intrathecal bolus: the leptomeningeal route for macromolecule and particle delivery to CNS. Molecular Pharmaceutics 2013, 10:1522-1532, DOI: 10.1021/mp300474m

### **Proceedings papers:**

M. Papisov, V. Belov, A.J. Fischman, J. Titus, M. Gagne, P. Calias, T. McCauley, M. Heartlein. Delivery of enzyme replacement therapeutics to CNS in rats and monkeys as seen and measured by PET. 39th Annual Meeting of the Controlled Release Society, Quebec, Canada, July 2012

Belova E, Vallance L, Belov V, Gagne M, Gillooly C, Papisov M. PET-based approaches to studying the size-dependence of leptomeningeal drug clearance. 39th Annual Meeting of the Controlled Release Society, Quebec, Canada, July 2012.

Belov V, Papisov M. A PET based method for real time monitoring of drug concentration in the liquid phase of the leptomeningeal compartment. 39th Annual Meeting of the Controlled Release Society, Quebec, Canada, July 2012.

Papisov M.I., Belov V., Fischman A.J., Titus J., Gagne M., Gillooly C., Bonab A., and Levine D. Physiology of intrathecal bolus as revealed by quantitative PET studies. 41st Annual Meeting of the Controlled Release Society, Chicago, IL, July 2014.

# Delivery of proteins to CNS as seen and measured by positron emission tomography

Mikhail I. Papisov · V. Belov · A. J. Fischman ·  
E. Belova · J. Titus · M. Gagne · C. Gillooly

Published online: 16 June 2012  
© Controlled Release Society 2012

**Abstract** Presently, there are no effective treatments for several diseases involving the central nervous system (CNS). While several novel molecular approaches are being developed, many of them require delivery of macromolecular or supramolecular agents to the CNS tissues protected by the blood–brain and blood–arachnoid barriers. Approaches that are being developed for overcoming these barriers are based on complex transport processes. The delivery of biopharmaceuticals and other molecules and particulates to the CNS, especially via the leptomeningeal (intrathecal) route, includes several stages, such as leptomeningeal propagation, drainage into systemic circulation, and penetration into the CNS. The investigation of complex pharmacokinetics that includes convective, as well as diffusional and active transfer processes, greatly benefit from real-time non-invasive in vivo monitoring of the drug transport. Pharmacological positron emission tomography (PET) imaging, which enables such monitoring, plays an increasingly significant role in drug delivery and biopharmacology. PET is a powerful tool for quantitative in vivo tracking of molecules labeled with positron-emitting radionuclides. The high sensitivity,

format, and accuracy of the data (similar to those of conventional tissue sampling biodistribution studies) make PET a readily adoptable pharmacological technique. In contrast to the conventional studies, PET also allows for longitudinal nonterminal same-animal studies. The latter may not only improve the data statistics, but also enable preclinical studies that are usually in large and/or rare animals) not feasible with the conventional approach. This paper is intended to describe the character of data that can be obtained by PET to demonstrate how the main patterns of the leptomeningeal route pharmacokinetics can be investigated by this method. Examples of data processing are taken from recent studies of five model proteins in rats and nonhuman primates.

**Keywords** PET Imaging · Pharmacokinetics · Biopharmaceuticals · Macromolecules · Brain · Central nervous system · Drug delivery · Iodine-124

## Introduction

The leptomeningeal route to the central nervous system (CNS) starts from drug administration (injection or infusion) into the cerebrospinal fluid (CSF) at one of the clinically feasible locations. The latter generally include lumbar spinal region and brain ventricles. Intrathecal lumbar (ITL) administration can be carried out via either needle insertion through an intervertebral disk or a surgically implanted catheter equipped with a subcutaneous injection port or a pump. Intracerebroventricular (ICV) administration is carried out through a surgically implanted cannula connected to an injection port anchored to the skull.

M. I. Papisov (✉) · V. Belov · E. Belova · J. Titus · M. Gagne ·  
C. Gillooly  
Massachusetts General Hospital,  
Bartlett Hall 500R, 55 Fruit Street,  
Boston, MA 02114, USA  
e-mail: papisov@helix.mgh.harvard.edu

M. I. Papisov · V. Belov · A. J. Fischman · E. Belova  
Harvard Medical School,  
Boston, MA, USA

M. I. Papisov · V. Belov · A. J. Fischman · E. Belova  
Shriners Hospitals for Children-Boston,  
Boston, MA, USA

Upon mixing with CSF, the drug is then transported with the latter and can be either delivered to the target CNS tissues (brain, spinal cord, and nerve routes) or drained to the systemic circulation along with CSF in which it is dissolved.

The interface of CSF with CNS is not protected by any barriers. The layer of pia mater lining the brain surface is not continuous, and the continuity of the leptomeningeal space with the perivascular (Virchow–Robin) spaces penetrating deep into the parenchyma [1] is the major prerequisite for the potential efficacy of this delivery route. The leptomeningeal route includes the following major transport stages: (a) convectional transport in the CSF, (b) drug penetration into the brain parenchyma and spinal cord, (c) transport inside the CNS tissues, (d) drainage outside of the leptomeningeal compartment, and (e) uptake by cells lining the leptomeningeal space or otherwise residing therein. The fraction of the drug reaching the target region(s) in the CNS depends on the kinetics of all these processes.

The ITL drug delivery route was originally developed for small molecules, primarily anesthetics [2]. The behavior of macromolecules and nanoparticles in the leptomeningeal space has not been extensively studied. Thus, the leptomeningeal route to CNS, although promising due to the absence of a CSF–CNS barrier, consists of processes that depend on many insufficiently studied (for large molecules and nanoparticles) factors working at various levels and on different time frames, such as, remixing of CSF by the pulsatile movement of CNS tissues, drainage of CSF, and intraparenchymal transport.

Investigation of the complex combinations of transfer processes, as above, would benefit from methods enabling: (1) whole-body quantitative registration of all transfer processes on all time frames; (2) real-time data acquisition in the same animal; and (3) using any animal as its own control, which removes the individual variances from the kinetic data.

Positron emission tomography (PET), as a powerful tool for quantitative in vivo imaging of the transport of pharmaceuticals labeled with positron-emitting radionuclides, meets the above requirements. With the growing number of drugs and drug delivery systems that have nontrivial pharmacokinetics, PET imaging will play an increasingly significant role in preclinical (especially nonhuman primate) and, possibly, human studies.

The present studies were intended to investigate the pharmacokinetics of human recombinant enzymes after intrathecal (IT) administration in rats and nonhuman primates, to evaluate the relevance of rodent vs. primate models, and develop methodology for fully quantitative non-invasive pharmacokinetics studies by PET with  $^{124}\text{I}$ .

## Experimental methods

### Imaging principles

Radionuclide-based imaging methods generally surpass all other in vivo imaging methods in sensitivity, and presently deliver enough resolution to delineate small organs in humans and experimental animals, including rodents. However, PET, which is based on a photon pair registration principle [3], has two technical advantages that make it superior to methods based on single photon acquisition.

In all radionuclide-based methods, the image is built on the basis of the experimentally acquired set of “lines” (lines of response or LORs in PET), along which each gamma photon has traveled before hitting a detector (a scintillating crystal).

In single-photon methods, i.e., planar imaging and gamma photon emission tomography (SPECT), the lines are defined via the use of collimators—metal (usually lead) blocks with channels, absorbing all photons except the ones traveling along the channels (Fig. 1). In planar imaging, a 2D image is formed essentially from the density of scintillations in the collimator crystal. In SPECT, the collimator/detector pair (“head”) rotates around the source of radiation, and a 3D image is reconstructed from the acquired set of lines.

In PET (Fig. 2), gamma photons are produced as a result of annihilation of the positron emitted by the radionuclide used as a label. Annihilation results in two gamma photons with peak energy of 511 keV, traveling in exactly opposite directions. Simultaneous detection of the pair by two detectors (the latter usually positioned as a set of rings) produces the LOR. The method does not require a collimator and, thus, is much more sensitive than single-photon modalities, where photon loss in the collimator generally exceeds 99 % (higher at higher resolutions). Photon scatter in the

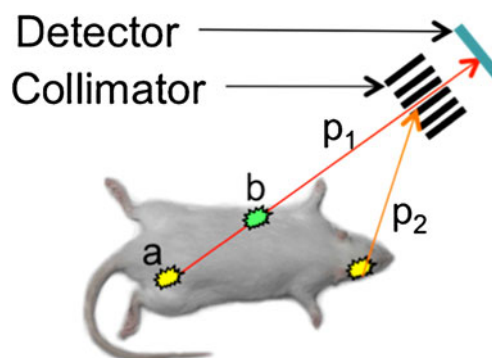


**Fig. 1** Single-photon data acquisition. The detector registers only gamma photons ( $p_1$ ) coming along the lines defined by the collimator, while other photons ( $p_2$ ) are absorbed. It is impossible to determine whether photon  $p_1$  came from point  $a$ , or point  $b$ , or any point in between. Thus, it is impossible to correct the data for photon absorption (attenuation) in the tissues

collimator is another factor complicating image formation in single-photon modalities.

The major advantage of PET, however, is in the relative simplicity of accounting for photon absorption in the tissues (attenuation). It is easy to see (Figs. 1 and 2) that there is no way of knowing from which point on the LOR a photon has come. Thus, in single-photon modalities, it is impossible to correct the data for absorption. In PET, the photons (as a pair) always pass the entire segment of LOR located between the detectors. Photon absorption in this segment can be easily measured experimentally, and thus the data can be readily corrected for attenuation. The attenuation data is produced from transmission images obtained using a rotating gamma radiation source or (in PET-computed tomography (CT)) from X-ray transmission data acquired by an X-ray CT imager.

There are several less significant differences in the data collection and processing, in particular those affecting resolution and artifact formation, but they are outside the scope of this paper. The combination of higher sensitivity and quantitative data acquisition are the two major advantages of PET. The quality of PET data (for a given tomograph), in turn, depends on many other factors, in particular on the positron emitting radionuclide used in the studies.

#### Iodine-124 as PET label

Imaging of slow PK, which is characteristic of many “large molecule” drugs and drug delivery systems, requires positron-emitting labels (radionuclides) with long physical half-lives.  $^{18}\text{F}$  is by far the most widely used positron emitter due to the high diagnostic value of clinical PET imaging with [ $^{18}\text{F}$ ]-fluorodeoxyglucose. However, the

physical half-life of  $^{18}\text{F}$  is only 110 min. To date, there are no satisfactory methods for labeling biomolecules (in aqueous phase) with this radionuclide. Thus,  $^{18}\text{F}$  is a suboptimal choice for studies requiring long (>5–6 h) observations. Other radionuclides used in PET imaging,  $^{11}\text{C}$ ,  $^{13}\text{N}$ ,  $^{15}\text{O}$ ,  $^{82}\text{Rb}$  and  $^{68}\text{Ga}$ , have even shorter physical half-lives: 20, 10, 2, 68, and 1.3 min, respectively. Copper-64 has a somewhat longer physical half-life (12.7 h) and can be used for labeling of compounds premodified with a chelating group, but the insufficiently studied fate of the label in vivo after metabolism of the labeled compound presently makes it useful mostly for studying of the early stages of biomolecules pharmacokinetics.

Recently,  $^{124}\text{I}$ , a cyclotron-produced radionuclide, has become commercially available. Among positron emitters available and suitable for PET,  $^{124}\text{I}$  has the longest physical half-life of 4.2 days. This, combined with the well-investigated behavior of iodinated biomolecules and iodide in vivo [4–6], makes  $^{124}\text{I}$  very attractive for long-term (several days) imaging studies.

The decay scheme of  $^{124}\text{I}$  is complex; its emission spectrum includes high-energy positrons (23 %) and high-energy single photons (60.5 % at 603 keV). Both the high energy of the positrons and the presence of single photons in the range close to the 511 keV of annihilation photon pairs may lead to degradation of sensitivity, spatial resolution, and image quality. However, we have shown that proper use of  $^{124}\text{I}$  provides fully quantitative data suitable for pharmacological research [7]. Therefore,  $^{124}\text{I}$  (IBA Molecular, VA, USA) was the main radionuclide in our studies. The radionuclide was supplied in the form of sodium  $^{124}\text{I}$  solution in 0.02 M NaOH, 0.3–2.7  $\mu\text{L}/\text{MBq}$ . Nominal radiochemical purity: 95 % (<5 % of iodate and diiodate by high-performance liquid chromatography (HPLC)). Nominal radionuclidic purity is >99 % at calibration (<0.5 % of  $^{123}\text{I}$ ;  $^{125}\text{I}$ : none detected, by HPGe gamma spectroscopy). Chemical purity is  $\text{Te} < 1 \mu\text{g}/\text{mL}$  by UV–VIS spectroscopy.

#### Enzymes and labeling

Three human recombinant enzymes, idursulfase, arylsulfatase A, and sulfamidase, were produced and characterized by Shire HGT. The proteins were labeled with  $^{124}\text{I}$  up to 185 MBq/mg and administered at various doses, via intravenous and intrathecal routes, in rats and (the former two proteins) in cynomolgus monkeys.

Protein labeling was carried out via direct iodination in the presence of Iodogen (Thermo Scientific Pierce, IL, USA). The iodination procedure was optimized for each protein to ensure >95 % radiochemical purity with preservation of enzyme structure, activity, and cell uptake characteristics. After the labeling, the proteins were briefly treated with metabisulfite (1 mg/ml, 1 min) to reduce iodoamines,

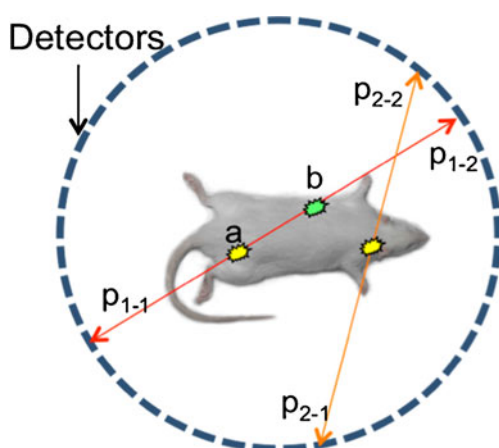


**Fig. 2** Photon pair data acquisition in PET. Positron annihilates with emission of two gamma photons traveling in opposite directions along the same line. It is impossible to determine whether photon pair  $p_{1-1}/p_{1-2}$  came from point  $a$ , or point  $b$ , or any point in between. However, it is possible to correct the data for photon absorption in the tissues based on experimentally determined attenuation values

desalted on Sephadex G-25, and characterized by size exclusion HPLC with dual (gamma, UV) detection.

### Imaging equipment

Imaging was carried out using either microPET P4 primate PET scanner (Concorde Microsystems/Siemens, TN, USA), or a custom PET/CT imaging system consisting of a MicroPET Focus 220 PET scanner and a CereTom NL 3000 CT scanner (Neurologica, MA, USA). In the latter system, the imagers were aligned and equipped with a custom imaging bed extending through both imagers along the alignment axis, ensuring reliable PET/CT image registration [8].

Both microPET P4 and Focus 220 worked in 3D mode and featured a 22 cm animal opening, axial field of view (FOV) 7.6 cm and transaxial FOV 19 cm. The scanner's detection systems enabled 2.5 mm (P4) and 2.1 mm (Focus 220) spatial resolution for  $^{124}\text{I}$ . The energy window of the PET imagers was set for the entire study to 350–650 keV, and the coincidence timing window was set to 6 ns.

CereTom NL 3000 is a six-slice tomograph with high-contrast resolution of 0.4 mm (developed for human head imaging in ICU). The image acquisition settings were: tube voltage, 100 kV; tube current, 5 mA; resolution, 6 s/projection; and axial mode with slice thickness of 1.25 mm. Image pixel size was set to  $0.49 \times 0.49 \times 1.25$  mm. The image sharpness was optimized to soft tissue. CT images were used for both anatomical reference and attenuation correction of the PET images. Fiducial markers (Eckert&Ziegler, Germany) were employed for PET/CT image co-registration that was carried out manually using ASIProVM software (Siemens/CTI Concorde Microsystems, Knoxville, TN, USA).

PET data acquisition, histogramming, and reconstruction were executed with the aid of microPET software (Siemens Medical Solutions, Inc., Malvern, PA, USA). Corrections for isotope decay, detector dead time, random coincidences, and tissue attenuation were applied. CT image reconstruction was carried out using Neurologica software. All subsequent image processing and analysis were performed on nonhost workstations using the ASIProVM software running under 32-bit Windows XP and Inveon Research Workplace 3.0 (Siemens Medical Solutions, Inc., Malvern, PA, USA) running under 64-bit Windows XP.

The PET data were reconstructed using a 3D ordered-subset expectation maximization/maximum a posteriori (OSEM3D/MAP) protocol with the smoothing resolution of 1.5 mm, nine OSEM3D subsets, two OSEM3D, and 15 MAP iterations. The data were also reconstructed with Fourier rebinning 2D filtered backprojection (FORE-2DFBP) [9] to ensure that the numerical data derived from OSEM3D/MAP and FORE-2DFBP reconstructed images were identical and thus to exclude the possible reconstruction artifacts

(none were identified). FORE-2DFBP was performed with a ramp filter cutoff at the Nyquist spatial sampling frequency ( $0.5 \text{ mm}^{-1}$ ). Whole body images were assembled of the acquired section images with a 12 mm overlap.

### Animals

All animal studies were carried out in accordance with institutionally approved animal protocols.

### Rats

**IV administration** Animals were set in a restrainer. A heparinized 3" catheter (BD 387334) was inserted into the tail vein and connected with a T connector (Abbott 1157218). Sodium pentobarbital, 35 mg/kg, was injected through the T connector cap and flushed with 0.5 mL saline. Then, animals were set on a MicroPET bed and injected with  $^{124}\text{I}$ -labeled model protein through the T connector cap (flushed with 0.5 mL of saline) simultaneously with the start of dynamic imaging procedure.

**IT administration** Animals were anesthetized with sodium pentobarbital (50 mg/kg, IP injection). Nonsurgical intracisternal injection was carried out using a technique developed by Jeffers and Griffith [10]. Immediately after the injection, rats were placed on the MicroPET bed, and data were acquired for the cranial region for 20 min.

### Nonhuman primates

Over the entire duration of the study, the animals were segregated from other NHPs and housed in a separate room at the MGH primate facility. At the housing site, the animals were sedated with Ketamine/Xylazine IM and then transported to the imaging site, where the animals were temporarily housed in standard NHP cages.

At the imaging site, each animal was first sedated with Ketamine IM (if and as needed), positioned on a custom polycarbonate imaging bed (MicroPET P4) or extended Focus 220 bed, and given continuous Isoflurane/ $\text{O}_2$  anesthesia. Heart rate, breathing rate, and  $\text{CO}_2$  content in the exhaled air were monitored continuously; isoflurane flow was adjusted as needed. Animals were given non-radioactive iodine (0.2 mL, 15 mM NaI) as a SC injection immediately before the study to suppress  $^{124}\text{I}$  uptake in the thyroid. The radioiodinated proteins were administered intravenously (IV) or intrathecally.

**IV administration** A catheter equipped with a T connector was installed in the saphenous vein. The animals were set on

a MicroPET bed and positioned for dynamic imaging of the lower thoracic (heart and liver) area. A transmission image was acquired before the injection. Then, the protein solution was administered through the T connector cap and flushed with 1 ml saline simultaneously with the start of the dynamic imaging procedure.

**ITL administration (direct injection)** The animals were sedated; the injection point was shaved, wiped with 70 % alcohol, and treated with Betadine. Injections were carried out in a prone position with a support providing a vertically bent, exposed injection area (atlanto-occipital joint for ICM, L4-L5 area for IL). A 27 G 1" needle equipped with a 3" transparent catheter with a T-cap was inserted between the vertebra until CSF flow is detected in the catheter. A small volume (0.1–0.2 mL) of CSF was drawn through the catheter. Then, the  $^{124}\text{I}$ -labeled model protein solution was injected through the T-cap, and the latter was flushed with 0.05 mL of the previously drawn CSF. The needle was withdrawn and the injection site was immediately imaged.

**ITL and ICV administration (catheterized animals)** The animals with surgically installed catheters equipped with subcutaneous injection ports (Northern Biomedical Research, MI, USA) were sedated; skin over the injection port wiped with 70 % alcohol, and treated with Betadine. Animals were set on the imaging bed in supine position. Injections were carried out through a 27 G 1" needle equipped with a 3" catheter with a T-cap. A small volume (0.1–0.2 mL) of CSF was drawn through the catheter. Then, the  $^{124}\text{I}$ -labeled model protein solution was injected through the T-cap, and the latter was flushed with isotonic saline, 0.5 ml/kg body weight. The needle was withdrawn and the injection site was immediately imaged for 20 min.

Both rats and nonhuman primates were imaged following essentially the same procedure. First, data was acquired for 20 min for the body section including the injection site (or catheter opening for ITL and ICV injections), and a section including the heart and the anterior edge of the liver. (The data was subsequently used for dynamic reconstruction). Then, full body section-by-section PET scans were carried out, 5 min (rats, monkeys) or 10 min (monkeys) per body section. Scans were performed on various schedules, in most studies at 1, 2, 4, 8, 24, 48, 96, and 192 h in rats and 1–5 h continuously with subsequent (12 or 24), (24 or 48), and 72 h points in monkeys. The data was subsequently used for static reconstruction. The numerical data from manually selected regions of interest were processed to determine protein concentration in the tissues.

## Other methods

Fluorescein isothiocyanate-labeled sulfamidase was utilized to investigate by photoimaging the microdistribution of the protein delivered to the brain in rats. The protein was injected into cisterna magna; animals were euthanized and the brains were cryosectioned 24 h after the injection. The cryosections were photoimaged (phase contrast, fluorescein 490/520 nm channel, custom blue 375/450 nm channel) without fixation or staining. Other control experiments were carried out in nonhuman primates (to be reported separately for each studied protein; partially published in [11]).

## Results and discussion

### Macromolecule transfer in CSF

The objective of our studies was to determine whether PET, as a quantitative imaging modality, could be used to investigate the general features of the leptomeningeal pharmacokinetics of macromolecules. Although the intrathecal route of drug delivery is not new, and vast data has been accumulated on the intrathecal administration of small molecules (mostly anesthetics), and several clinical applications have been successfully developed, both the properties of the prospective drugs and the mechanistic objectives of their delivery through the intrathecal route differ very significantly.

The main objective of the ITL administration of anesthetics is to achieve high drug concentration in the spinal cord and/or nerve roots locally to the injection point, whereas drug transfer to the cerebral leptomeningeal compartment can be detrimental to the subject (e.g., opiate drug transport to the respiratory center). In contrast, the target of enzyme replacement therapeutics and other macromolecular drugs is in the brain parenchyma, and their delivery to the cerebral leptomeningeal compartment is not undesirable but necessary.

The physicochemical properties of biomolecules generally should facilitate wide spread in the leptomeningeal compartment: they are too large to freely diffuse into the arachnoid and spinal cord parenchyma, and too hydrophilic to interact with the lipidic components of the tissue. Consequently, their behavior in CSF is expected to be entirely different from most anesthetics. On the other hand, the functions of the mesothelial and other cells have not been studied enough to predict how rapidly they will take up certain biomolecules dissolved in CSF. The flows and fluxes of CSF were also not sufficiently studied to predict how rapidly and in what directions biomolecules can be propagated in the leptomeningeal compartment from the injection site (ITL or ICV), although it is clear

that, considering the size of the molecules, diffusion cannot be expected to play a significant if any role in this process.

PET data demonstrated that in rats, all intracisternally administered proteins rapidly (within 5 min) spread over the entire cerebral CSF volume and into the proximal spinal leptomeningeal compartment (Fig. 3). In monkeys, the distribution process was dependent on the administered volume. Subcutaneous port administration generally suggests port flushing with relatively large volumes to ensure that the internal space of the port does not retain any significant fraction of the injected drug. The required volume for the ports used in this study (P.A.S. Port Elite, Smiths Medical ASD, Inc., MN, USA) to achieve <1 % dose remaining in the port was found to be about 1 ml. This is probably because the flush volume mixes with, rather than displaces, the internal port volume. Since the studies were carried out in animals with a wide range of body weights, from approximately 2–5 kg, the flush volume was adjusted for body weight to achieve the same intraspinal flushing effect in large animals as in smaller ones and was equal to 0.5 ml per 1 kg body weight. This is well below the injection volume that, as literature data suggests, is safe for primates,

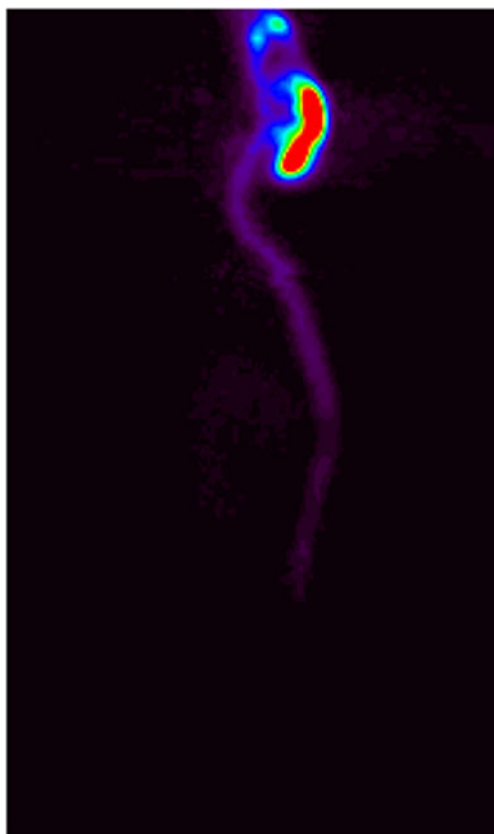


**Fig. 3** Distribution of idursulfatase in rat 1 h after intracisternal administration. Dose, 10 mg/kg. Projection PET image (the sum of all sagittal slices). Relative color scale

both human and nonhuman (up to 30 % of the total estimated CSF volume [11]).

According to our data, lumbar protein administration with 0.5 ml/kg body weight port flush (monkeys), which is <20 % of the estimated CSF volume, results in the immediate transfer of  $55 \pm 20$  % of the injected dose to the cerebral CSF. The movement of the protein in the spinal CSF is predominantly in the cranial direction, presumably because cranial and spinal leptomeningeal compartment (surrounded by bones) are not expandable, and the only expandable region of the dura is located in the cervical area, which accommodates the added volume.

Based on the imaging data, by 1–3 h, the administered protein fills all minor channels and tissue folds (Fig. 4). Lumbar administration in smaller volumes results in a slower but still efficient protein transfer to the cerebral CSF without deposition at the catheter opening site (Fig. 5, top). Visual analysis of the image shows that the protein spreads in both directions from the injection point, much faster than may be expected from a diffusion-based mechanism. We hypothesize that the transfer is convective and is assisted by pulsatile movement of the arteries in the leptomeningeal space and CNS tissues.

Figure 5 (bottom) is a numerical graphic representation of the same data as is in the images. The graphs represent the amount of protein in the leptomeningeal compartment per unit of length of the spine from neck (left) to dorsal area. As can be clearly seen in the dorsal region, the rate of translocation of the “front” of the protein in the dorsal direction in this particular animal exceeds 10 mm per hour, which cannot be explained by diffusion, but is in agreement with the propagation of protein in CSF through constant remixing of CSF by local turbulences induced by the pulsation of tissues. In humans, the layer of CSF is thicker than in nonhuman primates, and the rate of propagation can be expected to be higher (which is important for the pharmacokinetics of ITL administered drugs and require farther investigation).

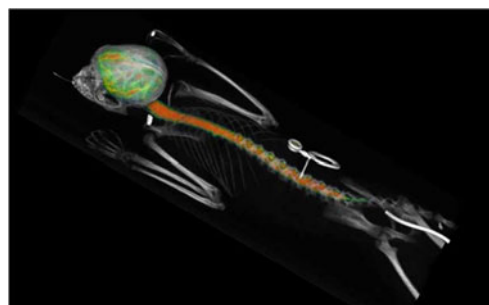


**Fig. 4** Protein distribution 3 h after ITL administration through a subcutaneous port (*center*) connected through a subcutaneous catheter with the leptomeningeal space. PET/CT image. Color represents 3D map of the protein concentration as measured by PET

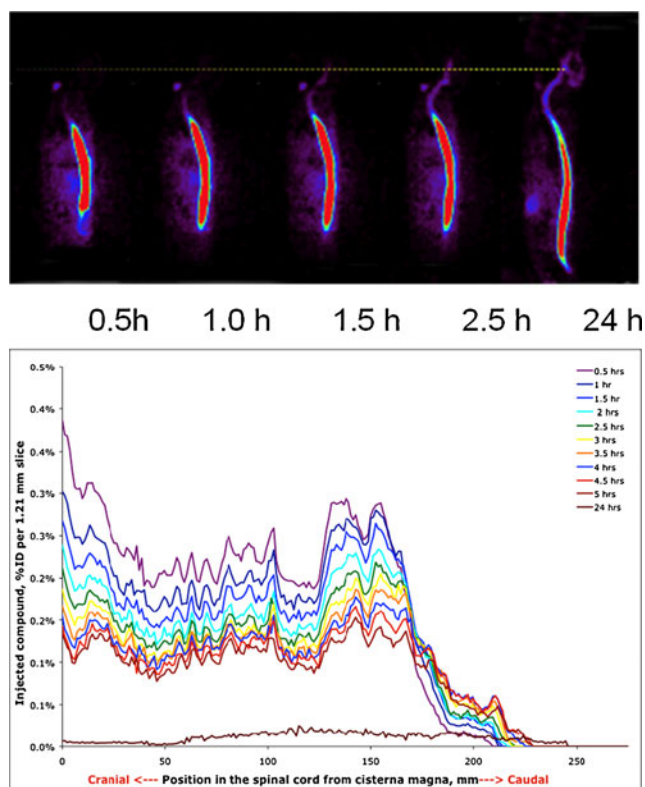


**Fig. 5** *Top* visual representation of PET data on idursulfase (10 mg/animal) spread from the lumbar injection point in a monkey (color concentration). *Bottom* numerical graphic representation of the same data (% of ID per unit of spine length as a function of time)

The data in Fig. 5 suggests that the uptake of the administered idursulfatase by the leptomeningeal tissues is relatively low. However, this may not be predictive of the behavior of other biomolecules. Detailed data on the receptor-specific endocytosis in the leptomeningeal space would be of great value for the development of drugs intended for the leptomeningeal route.

Protein injected ICV rapidly (within 15 min) translocated into the cisternae and basal channels (Fig. 6). The resultant protein distribution in CSF was very similar to that of large volume ILT administration without the deposition in the distal spine (Fig. 7a, described in more detail in our earlier publication [12]). Thus, notwithstanding some previous data [13], there is apparently no significant CSF descent (contrary to the pulsatile remixing of CSF), at least in this species. This, however, may be a matter of individual variations and may be influenced by pathological conditions as well as the nature of the labeled solute used in the studies. The issue of CSF movement (especially the general directions of the fluid flux vs. solute movements) as a result of local turbulences generated by pulsation, appears to be insufficiently studied and requires further investigation. PET, as a quantitative imaging modality, can be instrumental in such studies.

Thus, both ICV and ITL administration routes appear to enable efficient delivery of macromolecules to the cerebral leptomeningeal space. The kinetics of the delivery depends on the injection (and port flush) volume.

#### Macromolecule penetration from CSF into the brain parenchyma

**Rats** The small size of the rat brain prevented data analysis beyond calculating whole brain averages. For the three model enzymes, the label content in the brain was 45, 70, and 35 % after ITL administration for Idursulfase, arylsulfatase A, and sulfamidase, respectively (for comparison, IV administration resulted in 0.20, 0.15, and 0.05 % of injected dose/g, respectively). Idursulfase was cleared from both the brain and spinal cord with a half-life of ~7 h, while for the other two enzymes the half-life was ~24 h. Photoimaging studies indicated enzyme deposition in pia mater as well as in the brain parenchyma (not shown).

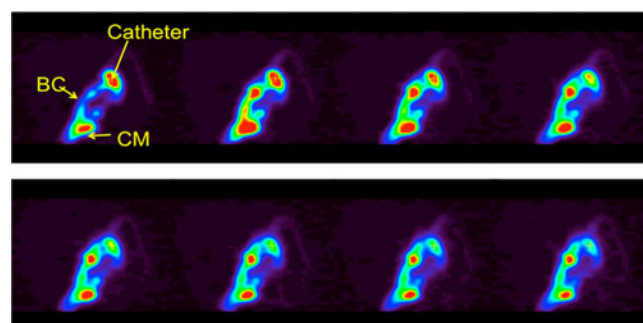
**Monkeys** In monkeys, protein penetration from CSF into the brain can be quantified from the imaging data in more detail due to the larger size of the brain. The rate of protein transfer was maximal during the first 2–5 h; by this time, a significant fraction (30–50 %, depending on the protein) was cleared from the CSF to the systemic circulation. Figure 7b illustrates the process of protein deposition in the brain for Idursulfatase.

Sequential PET imaging of the brain after the IT lumbar injection (Fig. 7b) demonstrated that I2S had moved from the CSF into the superficial (20–100 mcg/ml as estimated from PET data) and then into deeper brain tissues (3–20 mcg/ml). The inflow continued for 461 h, as exemplified by the differential (0.5–5 h) PET image in Fig. 7c. In the cranial segments, the clearance was faster (Fig. 7c), which is consistent with CSF drainage to the system predominantly in the arachnoid granulations of the superior longitudinal sinus [14]. No residual protein deposition was detected near the catheter opening.

Similar pharmacokinetics was observed for arylsulfatase and for nanoparticulate materials (not shown, will be published in detail elsewhere).

The mechanism(s) of protein translocation into the brain parenchyma from CSF require farther investigation. The rate of translocation suggests participation of active transport mechanisms. To date, PET and photoimaging data suggest that two mechanisms may be at work, (a) pulsation-assisted translocation along perivascular (Virchow–Robin) spaces [15] and (b) axonal transport [16].

**Fig. 6** Time course of ICV administration, 2 min per frame. PET dynamic reconstruction, sagittal slice through the catheter tip (*catheter*), central-basal channel (*BC*), and cisterna magna (*CM*)



### Macromolecule clearance from CSF

Transfer of proteins dissolved in CSF to the systemic circulation started immediately after the injection, without a lag, which is not consistent with CSF drainage to the lymphatic system with subsequent transfer to the blood, and suggests transfer directly to the blood.

Lymphatic transfer would also suggest protein accumulation in lymph nodes draining cerebral, cervical and spinal regions. Any lymphatic accumulation would be readily detectable by PET. However, none of the studied monkeys ( $n=20$ ) or rats ( $n=64$ ) demonstrated any lymphatic accumulation along the spine, with exception of single nodes sentinel to the lumbar injection sites. In monkeys, no significant

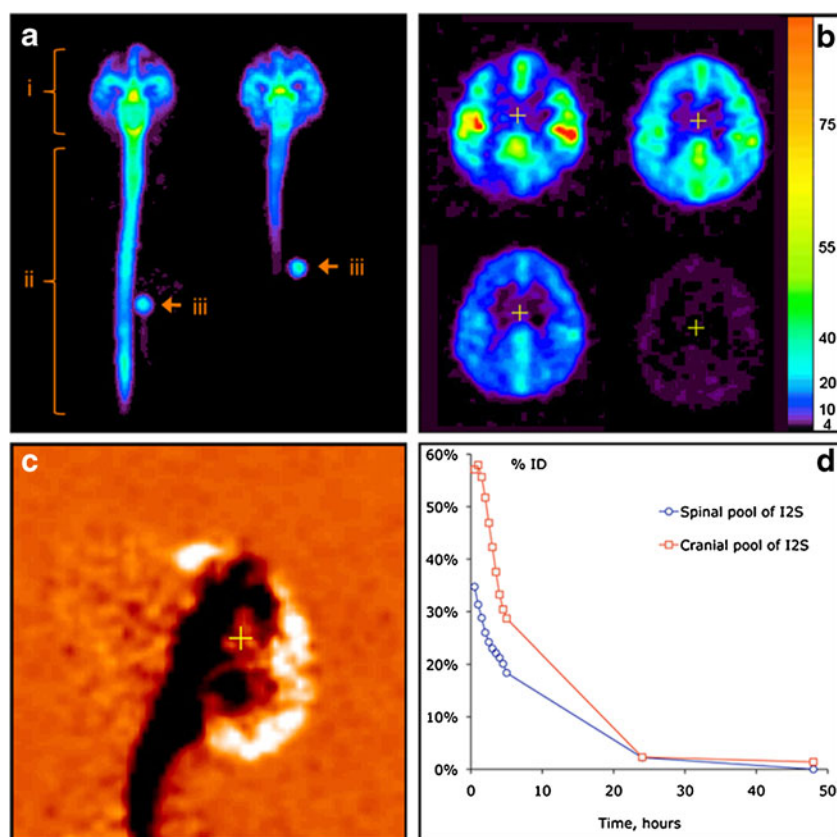


**Fig. 7** In vivo distribution of  $^{124}\text{I}$ -labeled I2S (3 mg/animal) in cynomolgus monkeys by PET. **(a)** Distribution of I2S administered through the lumbar (left) and ICV (right) catheters 30 minutes after the administration as demonstrated by a projection PET image (sum of all slices). Relative linear color scale. **(b)** The distribution of I2S in the brain at 0.5, 2.5, 5 and 24 hours after lumbar administration; PET image, 1.2 mm slice through the corpus callosum region in the plane parallel to the occipital bone. The color scale is calibrated in mg/ml of

I2S. **(c)** Changes in the cerebral I2S distribution between 0.5 and 5 hours after lumbar administration shown in monochrome linear color scale. The image was obtained by subtraction of the quantitative data matrix obtained at 5 hours from the one obtained at 0.5 hours. Neutral orange color represents no change. Clearance of I2S from the CSF is seen as black, and accumulation in the parenchyma and arachnoid as white color. **(d)** An example of single-animal dynamics of I2S clearance from the leptomeningeal compartment and CNS [12]

lymphatic accumulation was found in cervical lymph nodes as well. In rats, cervical and submandibular nodes showed some accumulation (generally <1 % of ID), but this could be a result of minor CSF leakages from the intracisternal injection sites and thus further investigation is necessary.

Thus, the PET data suggest that, at least in nonhuman primates, there is no physiologically significant CSF drainage into the lymphatic system, and in rats there is no such drainage from the spinal pool of CSF. This data further suggests that in primates, penetration of CSF through the cribriform plate into the olfactory epithelium is insignificant, because from there it would have to drain into the cervical lymph nodes, which has not been observed. There was no indication of significant radioactivity accumulating anywhere in or around the nasal airways at any time point as well.

Thus, the kinetics of protein drainage from the leptomeningeal space is in the agreement with direct drainage with CSF to the blood (presumably in arachnoid villi) [14], and the rate of protein transfer to the systemic circulation is in agreement with the rate of CSF exchange [17] (Fig. 7d).

## Conclusions

PET provides a variety of image and quantitative data suitable for both visual and numerical analysis. Overall, our data demonstrate that the leptomeningeal (intrathecal) route is suitable and promising for protein delivery to the brain parenchyma, including both gray and white matter. Biologically significant levels of the studied proteins were found in all brain compartments. Considering the mechanistic context, this suggests that other macromolecules and nanoparticles may also be delivered to CNS via this route.

Several mechanistic aspects of leptomeningeal drug transport, such as parenchymal transfer, CSF drainage and mesothelial uptake, are important for understanding of the data, and warrants further investigation. The data demonstrate that the initial transfer of intrathecally administered proteins can significantly depend on the injection (and port flush) volume, which also warrants further investigation.

**Acknowledgments** This work was supported by NIH grant R21 CA152384, DoD grant BC100684, and grants from Shire HGT. Shire HGT also provided model proteins and imaging equipment.

## References

1. Rennels ML, Gregory TF, Blaumanis OR, Fujimoto K, Grady PA. Evidence for a paravascular fluid circulation in the mammalian central nervous system, provided by rapid distribution of tracer protein throughout the brain from the subarachnoid spaces. *Brain Res.* 1985;326:47–63.
2. Yaksh T, editor. *Spinal drug delivery*. Amsterdam: Elsevier; 1999.
3. Sweet WH, Brownell GL. Localization of brain tumors with positron emitters. *Nucleonics.* 1953;11:40–5.
4. Friedman JE, Watson Jr JA, Lam DW-H, Rokita SE. Iodotyrosine deiodinase is the first mammalian member of the NADH oxidase/flavin reductase superfamily. *J Biol Chem.* 2006;281:2812–9.
5. Ullberg S, Ewaldsson B. Distribution of radio-iodine studied by whole-body autoradiography. *Acta Radiol Ther Phys Biol.* 1964;2:24–32.
6. Hays MT, Solomon DH. Influence of the gastrointestinal iodide cycle on the early distribution of radioactive iodide in man. *J Clin Invest.* 1965;44:117–27.
7. Belov VV, Bonab AA, Fischman AJ, Heartlein M, Calias P, Papisov MI. Iodine-124 as a label for pharmacological PET imaging. *Mol Pharm.* 2011;8(3):736–47.
8. Carney JPI, Flynn JL, Cole KS, Fisher D, Schimel D, Via LE, Cordell M, Longford CPD, Nutt R, Landry C, Tybinkowski AP, Bailey EM, Frye LJ, Laymon CM, Lopresti BJ. Preclinical PET/CT system for imaging non-human primates. *IEEE Medical Imaging Conference.* 2009; abstract M06-67.
9. Defrise M, Kinahan PE, Townsend DW, Michel C, Sibomana M, Newport DF. Exact and approximate rebinning algorithms for 3-D PET data. *IEEE Trans Med Imag.* 1997;16:145–58.
10. Farris, Griffith, editors. *The rat in laboratory investigation*. Philadelphia: Lippincott; 1949. p. 196–7.
11. Rieselbach RE, Di Chiro G, Freireich EJ, Rall DP. Subarachnoid distribution of drugs after lumbar injection. *N Engl J Med.* 1962;267:1273–8.
12. Calias P, Papisov M, Pan J, Savioli N, Belov V, et al. CNS penetration of intrathecal-lumbar idursulfase in the monkey, dog and mouse: implications for neurological outcomes of lysosomal storage disorder. *PLoS One.* 2012;7(1):e30341. doi:10.1371/journal.pone.0030341.
13. Chiro GD, Hammock MK, Bleyer WA. Spinal descent of cerebrospinal fluid in man. *Neurology.* 1976;26:1–8.
14. Segal MB. Fluid compartments of the central nervous system. In: Zheng W, Chodobski A, editors. *The blood–cerebrospinal fluid barrier*. Boca Raton: CRC; 2005. p. 83–99.
15. Rennels M, Gregory TF, Blaumanis OR, Fujimoto K, Grady PA. Evidence for a paravascular fluid circulation in the mammalian central nervous system, provided by the rapid distribution of tracer protein throughout brain from the subarachnoid space. *Brain Res.* 1985;326:47–53.
16. Passini MA, Lee EB, Heuer GG, Wolfe JH. Distribution of a lysosomal enzyme in the adult brain by axonal transport and by cells of the rostral migratory stream. *J Neurosci.* 2002;22:6437–46.
17. Davison H, Segal MB, editors. *Physiology of the CSF and the blood–brain barriers*. Boca Raton: CRC; 1996. p. 201.

# Physiology of the Intrathecal Bolus: The Leptomeningeal Route for Macromolecule and Particle Delivery to CNS

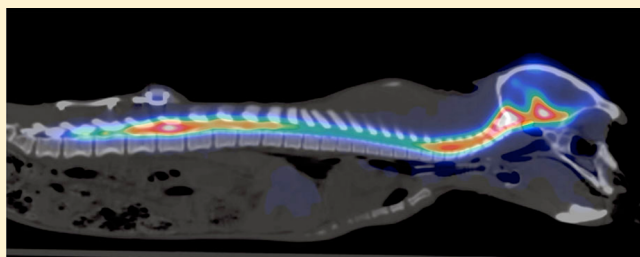
Mikhail I. Papisov,<sup>\*,†</sup> Vasily V. Belov,<sup>†</sup> and Kimberley S. Gannon<sup>‡</sup>

<sup>†</sup>Massachusetts General Hospital, Shriners Hospitals for Children—Boston, and Harvard Medical School, 51 Blossom Street, Boston, Massachusetts 02114, United States

<sup>‡</sup>NeuroPhage Pharmaceuticals, Inc., 222 Third Street, Suite 3120 Cambridge, Massachusetts 02142, United States

**ABSTRACT:** Presently, there are no effective treatments for several diseases involving the CNS, which is protected by the blood–brain, blood–CSF, and blood–arachnoid barriers. Traversing any of these barriers is difficult, especially for macromolecular drugs and particulates. However, there is significant experimental evidence that large molecules can be delivered to the CNS through the cerebrospinal fluid (CSF). The flux of the interstitial fluid in the CNS parenchyma, as well as the macro flux of CSF in the leptomeningeal space, are believed to be generally opposite to the desirable direction of CNS-targeted drug delivery. On the other hand, the available data suggest that the layer of pia mater lining the CNS surface is not continuous, and the continuity of the leptomeningeal space (LMS) with the perivascular spaces penetrating into the parenchyma provides an unexplored avenue for drug transport deep into the brain via CSF. The published data generally do not support the view that macromolecule transport from the LMS to CNS is hindered by the interstitial and CSF fluxes. The data strongly suggest that leptomeningeal transport depends on the location and volume of the administered bolus and consists of four processes: (i) pulsation-assisted convectional transport of the solutes with CSF, (ii) active “pumping” of CSF into the periaxonal spaces, (iii) solute transport from the latter to and within the parenchyma, and (iv) neuronal uptake and axonal transport. The final outcome will depend on the drug molecule behavior in each of these processes, which have not been studied systematically. The data available to date suggest that many macromolecules and nanoparticles can be delivered to CNS in biologically significant amounts (>1% of the administered dose); mechanistic investigation of macromolecule and particle behavior in CSF may result in a significantly more efficient leptomeningeal drug delivery than previously thought.

**KEYWORDS:** CNS, intrathecal, leptomeningeal, cerebrospinal fluid, CSF, drug delivery, biopharmaceutics, proteins, bacteriophage, drug carriers, imaging



## INTRODUCTION

Diseases involving the CNS are of high social significance due to high prevalence and/or high morbidity and mortality. Presently, there are no effective therapies for many of them, not least because of the poor drug access to the CNS. It has been estimated that, for greater than 98% of small molecules and nearly 100% of large molecules, systemic delivery to the CNS is not effective.<sup>1</sup> As a result, several conditions involving CNS remain untreatable. Examples include neurodegeneration (e.g., amyotrophic lateral sclerosis), “diseases of age” (Alzheimer’s and Parkinson’s diseases), genetic deficiencies (e.g., lysosomal storage diseases<sup>2</sup>), and several types of brain cancer (e.g., childhood brainstem glioma<sup>3</sup>).

If the problem of their delivery to CNS is solved, then biopharmaceutics (proteins,<sup>4–6</sup> oligonucleotides,<sup>7,8</sup> gene vectors<sup>9–11</sup>) may potentially provide highly effective therapies for many diseases involving the CNS. The attempts of circumventing or traversing the blood–brain barrier (BBB), including the use of direct transcranial administration and transport across the BBB using endogenous receptors (insulin, transferrin, LDL receptors, LDLR-related proteins)<sup>12–14</sup> and

nanocarriers,<sup>15</sup> hold significant promise but have not yet resulted in clinically accepted solutions.

The fact that large molecules can penetrate into the brain parenchyma from the cerebrospinal fluid (CSF) was established four decades ago.<sup>16</sup> However, only recently it has been shown that the fraction of therapeutic macromolecules or particles (gene vectors) delivered to the CNS from CSF may be biologically significant.<sup>17–23</sup> Our recent studies using PET as a method of noninvasive tracking of intrathecally administered proteins and particles, such as particles of bacteriophage M13 (below in the text “phage”),<sup>24–26</sup> have shown a high and rapid entrance into the brain parenchyma, which may appear surprising, considering the prevailing views on the physiology of the leptomeningeal space. (Leptomeningeal space (LMS) is

**Special Issue:** Drug Delivery across the Blood–Brain Barrier

**Received:** August 27, 2012

**Revised:** January 10, 2013

**Accepted:** January 14, 2013



understood here as the entire space occupied by CSF, including all spaces continuous with the subarachnoid space, such as perivascular spaces and ventricles.) This paper is intended to discuss the mechanistic aspects of the macromolecule and particle translocation in the leptomeningeal space and their role in the intrathecal delivery to the CNS, particularly to the brain.

The current clinical paradigm of leptomeningeal (intrathecal) drug administration is rooted in the pioneering work of J. Corning (1885) on spinal anesthesia with cocaine<sup>27</sup> and has been greatly influenced by the subsequent studies in anesthesiology, in particular investigating the risk of respiratory distress when the anesthetic is administered at a higher location than the lower thoracic area.<sup>28</sup> Recent significant developments were based on the recognition that hydrophobic anesthetics introduced in LMS induce rapid segmental anesthesia, while hydrophilic anesthetics induce more gradual onset of anesthesia, with actions extending from the administration site.<sup>29,30</sup> The published observations generally fit into the mechanistic scheme where the drug administered into the spinal CSF acts locally, being contained by its association with the lipids of the arachnoid and, presumably, by the hypothetical caudad CSF flow. The cephalad (upward) spread of an anesthetic from injection sites close to the head could be risky because of the proximity of the medullary vasomotor centers.<sup>31</sup> Thus, the development of intrathecal delivery of anesthetics was focused on slow infusion in the lumbar region. Coincidentally, due to the anatomy of the skull and vertebrae, lumbar administration is the most clinically feasible and least invasive way for drug introduction to the LMS. As a result, in anesthesiology the lumbar intrathecal administration has become prevalent. Implantable slow infusion devices have been developed, capable of chronic (years) uninterrupted delivery of pain or spasticity management therapies with the action focused mostly on the distal segments of the spinal cord.<sup>32,33</sup>

In other fields of medicine, the use of the leptomeningeal route for access to the CNS has not yet been systematically explored; the number of both preclinical and clinical studies where this route is tested is not very large. This, apparently, is partially due to the perceived (and likely overestimated) dependence of the drug transport in the CSF on the CSF "circulation"<sup>34</sup> and other perceived limitations.<sup>35</sup>

In several animal models of CNS disease the intrathecal drug delivery route has shown promising results for large molecules. This includes intrathecal delivery of enzyme replacement therapeutics,<sup>36,21,37–39</sup> antibodies,<sup>40</sup> nerve growth factor,<sup>41</sup> Sonic Hedgehog,<sup>42</sup> siRNA,<sup>43</sup> and dynorphins.<sup>44</sup>

One recent paper describing the results of early clinical studies states: "[Intrathecally administered] BDNF can be delivered cranially against CSF flow."<sup>45</sup> In fact, the most recent data suggest that the CSF "flow" is perhaps the least important factor of leptomeningeal transport of macromolecules. The solute transport in CSF, as discussed below, is much more influenced by the initial spread of the injected solution in the CSF, subsequent active transport of the solute in the LMS due to pulsatile remixing, drainage of the CSF outside the LMS, and active, pulsation-assisted translocation of the solute into the perivascular space (Virchow–Robin space, VRS), and the subsequent transfer from VRS to the parenchyma and uptake and transport by cells.

## THE ANATOMY OF THE LMS AND THE ROLE OF THE INJECTED VOLUME IN THE INITIAL DRUG SPREAD

The brain and spinal cord are suspended in the CSF-filled LMS on avascular membranes and ligaments (trabeculae), which are collectively called "arachnoid" due to their weblike appearance (Figure 1). On the outside, the membranes and trabeculae are attached to the dura: the outermost of the meninges. Dura is essentially a seamless sac containing the cerebrospinal fluid.

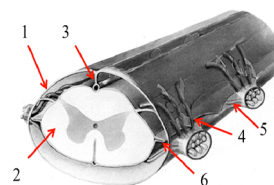


**Figure 1.** Internal structures of the leptomeningeal space. Dura (1), spinal cord (2), longitudinal membrane (3), dorsal and ventral nerve rootlets (4, 5), dorsolateral septum (6). Transverse membranes and the mesh of ligaments (trabeculae) are not shown. Reprinted with permission from ref 46. Copyright 1983 Elsevier.

Dura, for the most part, is surrounded by bones (skull, vertebrae) and relatively rigid cartilage (intervertebral disks) and thus has no space to expand (or contract). However, there are two exceptions to the latter: (a) the area ("cisterna magna") near the atlanto-occipital and atlanto-axial joints, where dura has to accommodate for the movements of the head and neck, and (b) to a lesser degree, intervertebral openings (foramina) through which nerves and blood vessels exit the LMS. The firmly confined boundaries of the LMS define the initial behavior of any additional liquid introduced to the CSF by injection. Thus, regardless of the injection site (e.g., cerebroventral, lumbar), the injected liquid will "push" the CSF toward the expandable area (and toward major veins that can contract and accommodate extra volume under pressure<sup>74</sup>) and spread toward the same direction, i.e., mainly toward the neck area. If the administered volume exceeds the volume of the compartment located between the injection site and the flexible section of the dura, the respective fraction of the dose is delivered directly into the cisterna magna area. The "distances" (expressed in volume units) between various potential injection points and cisterna magna in various animals can be measured experimentally either by CSF sampling or, preferably, non-invasively (by imaging). To the best of our knowledge, this still has not been done systematically. Rieselbach et al. administered large volumes of radiolabeled preparations into the lumbar sac, [<sup>131</sup>I] Rose Bengal in *Macaca mulatta* and [<sup>198</sup>Au] colloidal gold in human patients.<sup>47</sup> Their data suggest that in both humans and monkeys the administration of over 10% of the total estimated CSF volume results in the immediate appearance of the radioactivity in the intracranial CSF (cisterna magna and basal cisterns).

In our studies in cynomolgus monkeys (*Macaca fascicularis*), the estimated "distance" from the lumbar injection point (at L1) to cisterna magna was approximately 0.4 mL/kg of body weight; administration of a 0.5–1 mL bolus followed by a 0.5 mL/kg flush resulted in the immediate delivery of 50% of the administered dose to the cranial CSF pool for all studied proteins and particles.<sup>24–26</sup> Intracerebroventricular administration of the same protein resulted in a very similar initial protein

distribution pattern in the CSF. The pattern was significantly different only for the distal thoracic and lumbar regions, where the initial protein content was much lower than after lumbar administration.<sup>24</sup> We should note that the position of the needle or catheter opening relative to the spinal cord (dorsally or ventrally) may influence the apparent “distance” to the cisterna magna, because the ventral LMS is relatively open and the dorsal space is crossed by multiple membranes (Figure 1), the continuity and variability of which still have not been studied in detail.<sup>48</sup> Our current studies in rats suggest that catheter tip position can change the initial pattern of bolus translocation very significantly.<sup>49</sup>

Thus, the initial spread of the drug administered by bolus injection is defined by the anatomy of the LMS and depends on the injected volume. The influence of other physical factors (e.g., body position, reinjection) is unlikely to be important. Rieselbach et al. observed that withdrawal and reinjection of [<sup>198</sup>Au] did not unequivocally improve distribution in comparison with patients receiving a similar volume with one rapid injection,<sup>47</sup> which is not unexpected since withdrawal and reinjection only moves the solution back and forth along the same segment of LMS. We should note, however, that withdrawal of a CSF volume equal to the subsequently injected dose may result in a safer procedure due to the prevention of the excessive buildup of the CSF pressure (Rieselbach's data suggest that bolus injection of up to at least 33% and 42% of the total CSF volume is well tolerated by humans and monkeys, respectively).

The influence of the “baricity” (solution density as compared to the CSF) on the initial distribution of the injectate was first suggested by A. Barker<sup>50</sup> in 1907. He showed that “hyperbaric” (more dense than CSF) and “hypobaric” solutions (less dense than CSF) can flow under the influence of gravity in the spinal canal. Combined with various degrees of body tilt (Trendelenburg position), injection of air, and/or direction of the needle opening, this observation has resulted in various techniques for localizing the action of intrathecally administered anesthesia.<sup>51–53</sup> The feasibility of gravity-assisted transport of macromolecules and particles in the LMS has not been investigated.

Thus, the volume of the intrathecal bolus appears to be the most important factor of the initial drug spread in the CSF. After the initial distribution, or after the administration of a small volume, the solute distributes within the LMS relatively slowly. The mechanism and directionality of this distribution are discussed in the following section.

## ■ THE “FLOW” OF CSF

The CSF is believed to be produced mostly by the choroid plexus, a highly vascularized tissue located in the brain ventricles. The formation of CSF and the functions of choroid plexus are very well studied and extensively reviewed.<sup>54,55</sup> Approximately 18–20% of the CSF appears to originate from the interstitial fluid of the CNS in rabbits,<sup>56</sup> with higher interstitial contribution in non-human primates and other species.<sup>57</sup>

An early view suggested that the circulation of the fluid is a movement from its point of production toward the arachnoid villi to replace fluid which has been absorbed in this situation; later it was suggested that the cerebrospinal fluid circulation is aided by a vascular pump which drives fluid from the ventricles and through the cranial subarachnoid space.<sup>58</sup> Although there are alternative points of view,<sup>59</sup> it is generally accepted (Figure

2) that CSF flows from the ventricles into the basal channels and then into other cranial subcompartments of LMS.<sup>60,61</sup>

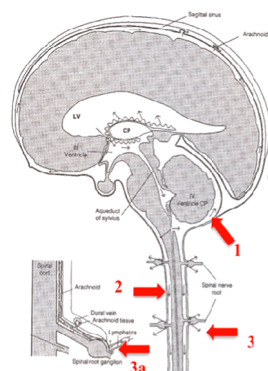


**Figure 2.** One of the most reprinted schemes depicting the “circulation and drainage” of CSF. Red arrows: examples of CSF “flows” the significance of which for drug delivery can be misinterpreted (see text). Reprinted with permission from ref 62. Copyright 1930 American Medical Association.

Early experiments with direct observation of the movement of dye administered to the CSF of laminectomized dogs resulted in the conclusion that there is no directional CSF flow.<sup>63</sup> In the same publication, the authors conclude that the substances in the CSF spread by diffusion and that there is no evidence that pulse and respiration play a role in the movement of CSF (we must note that the method was not precise enough to adequately support the latter conclusions).

In a later imaging study,<sup>64</sup> a descent of a radiolabeled solute in the spinal LMS was interpreted as descent of CSF; the interpretation remained uncontested.

For a drug administered in the lumbar region, a downward CSF flow direction in the spine would hinder the intended drug transport. Thus, it may appear that only a very small fraction of the intrathecally injected drug can reach the cerebral CSF pool and the brain surface. This view, however, does not take into account that the “flow” of the CSF is not laminar.

The pulsatile movements of the CSF, mainly in the cervical/ventricular area,<sup>74</sup> create longitudinal oscillations in the CSF along the entire LMS. Most recently, noninvasive flow measurement with phase contrast MRI enabled the *in vivo* evaluation of the basic parameters of this CSF movement, such as flow velocities and waveforms.<sup>65–69</sup> Computational flow dynamics (CFD) models have been used to complement MRI measurements in explaining the complex fluid flow patterns in the CSF-filled spaces.<sup>70–72</sup> Generally, CSF flow waveform reflects that of the arterial cardiac cycle and has its own systole (spinal column inflow) and diastole (outflow). Peak pulsatile flow rates measured at the cervical level by different authors<sup>65,66,72,73</sup> range from 120 mL/min to 360 mL/min in humans. The variations in the velocity are significant along the spinal canal and range from 0.5 to 8 cm/s with the maximum at ca. 20 cm below the skull.<sup>72</sup> CFD studies show that inertial effects should dominate the flow field causing significant turbulence, especially in the cervical LMS.<sup>66</sup>

In a turbulent liquid compartment, the flux of the solute is not necessarily governed by the bulk flux of the liquid. Turbulence induced in the CSF by the pulsation of the arteries and tissues can propagate the solute along the compartment when there is no solvent flux and even against the flux. For mechanistic reasons, it can be expected that in a small segment

of LMS the pulsatile movements should result in the solute flux proportional to the concentration gradient between the ends of the segment, in a simplified form,

$$J = k_{pd} \cdot \text{grad}(C) \quad (1)$$

where the “pseudodiffusion” constant  $k_{pd}$  is a function of the intensity and patterns of the local pulsatile turbulence. The form of this equation is similar to Fick’s diffusion equation; however, the underlying process is nondiffusional and does not depend on the hydrodynamic diameters of the solute molecules and particles. In studies performed using quantitative positron emission tomography (PET), the real-time in vivo data obtained using proteins and phage particles, which differed in size by about 2 orders of magnitude (ca. 12–14 and 900 nm, respectively), showed that in the distal spinal CSF of *M. fascicularis* the rate of solute transport is much higher than of diffusion, 0.3–2.1 cm/h for both smaller and larger solutes, as estimated by the front propagation (Figure 3); the range of

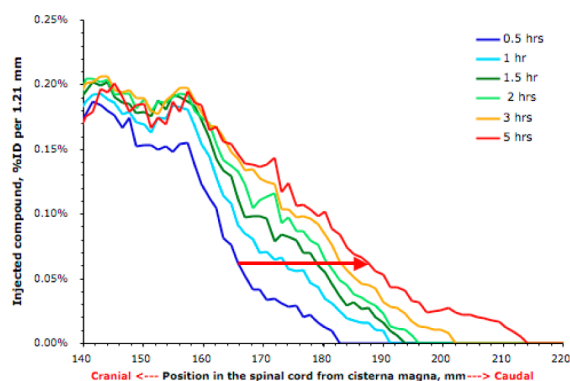


**Figure 3.** Solute front propagation in the distal lumbar section of the LMS: ca. 0.5–0.7 mm per hour in this animal (derived from data obtained in ref 26).

values reflects variations within the same animal’s LMS as well as between the animals. In rats, a very small volume (3  $\mu\text{L}$ ) injected at L1 region in the rat’s spine expanded both cranially (at ca. 2.8 cm/h) and caudally (at ca. 1.4 cm/h). As a result, the solute distributed over the entire spinal CSF of the rat within approximately 1 h.

Thus, the experimentally observed rates of solute transport in the CSF are by orders of magnitude faster than diffusional transport. On the other hand, the imaging data suggest that macromolecules (or particles) spread in the CSF from the administration point in all directions (e.g., to the cerebral LMS from the spine and to the spinal CSF from the ventricle), which excludes a directional CSF flux as the driving force. Therefore, the pulsatile remixing of CSF appears to be the main if not the only driving force in the macromolecule spread in the LMS.

The pulsatile turbulence of the CSF has a much more significant effect on the solute spread in the liquid phase than the CSF “flow” because the directional flux of the CSF is very slow as compared to the pulsatile remixing in all parts of the LMS that is responsible for the solute flux. The local turbulences of CSF, which drive the spread of the solute, are most intense in the area identified by Du Boulay et al.<sup>74</sup> and, respectively, lower (but not absent) where the arteries branch and become thinner, as shown in Figure 4.

The above suggests that a mechanistic pharmacokinetic model can be developed based on the physiology and

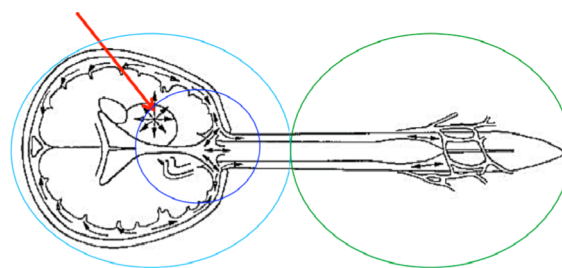


**Figure 4.** Scheme of the CSF remixing zones. Red arrow: the “CSF pump”:<sup>74</sup> pulsation of major arteries causes pulsatile contraction of the 3rd ventricle transmitted through the entire liquid compartment. Blue, light blue, and green areas: zones of very fast, slower, and very slow remixing of CSF, according to our PET data. These zones will have different  $k_{pd}$ . Graphics based on ref 75, with permission. Copyright 2011 Biomedical Engineering Society.

configuration of the leptomeningeal space, with parameters essentially based on eq 1. To the best of our knowledge, these parameters were never measured for any animal, although the approaches are presently being developed.<sup>74</sup> The availability of experimentally validated quantitative models for different species would greatly facilitate both preclinical development and translation to human studies.

The pool of the drug substance dissolved in the CSF may, during and after the initial distribution, further translocate into the CNS or out of the leptomeningeal space following the physiological avenues. Also, depending on the structure of the macromolecule or particle surface, the mobility of the drug substance in the LMS can potentially be attenuated by the molecule or particle interactions with cells lining the leptomeningeal tissue interfaces. Some of these cells may potentially bind or endocytose the drug. The mechanisms and rates of these processes, which may change in pathological states, are of key importance for the overall results of leptomeningeal transport, as discussed in the following sections.

## ■ DRAINAGE OF CSF

CSF drainage is a process that removes the excess of the fluid from the leptomeningeal space and maintains the leptomeningeal volume constant. The rate of fluid replacement varies in different species, from 0.89% of the total volume per minute in the mouse to 0.38% per minute in human.<sup>77</sup> The drainage routes have been investigated for nearly a century, but there are still conflicting views due to the significant methodological difficulties.<sup>78</sup>

The principal CSF draining route is believed to be in the venous sinuses through physical pores found in specialized structures, arachnoid granulations<sup>79</sup> (we must note the debate continues even now<sup>80</sup>). In humans and non-human primates, the arachnoid granulations were found in the superior sagittal and lateral sinuses,<sup>81</sup> and at some nerve roots,<sup>82</sup> while in rabbits they were found only at the cranial base.<sup>83</sup> In rats, the drainage site is in the superior sagittal sinus, although arachnoid granulations are not as defined as in other animals.<sup>84</sup> In the preparations of arachnoid granulations, multiple pores are apparently formed by merged giant vacuoles (Figure 5). Whether these channels are permanent or dynamic remains unknown. R. Tripathi<sup>85</sup> suggests that filtration proceeds through 0.1–2.3  $\mu\text{m}$  temporary openings of giant vacuoles, but makes no suggestions on the duration of the existence of such channels. In rats, the administered solute (peroxidase) was

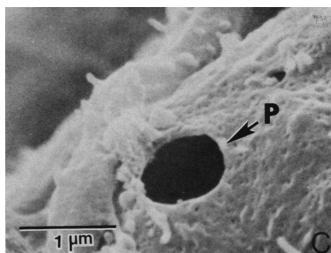


**Figure 5.** Leptomeningeal pore (P). Reprinted with permission from ref 76. Copyright 1995 CRC Press. Scanning electron micrograph.

also found in numerous transendothelial vesicles, suggesting a dual filtration mechanism.<sup>86</sup>

In addition to the direct drainage, paraneural CSF drainage into the interstitium with subsequent lymphatic drainage was suggested (as shown, in particular, in Figure 2, arrows 3 and 3a), e.g., in rabbits.<sup>87</sup> The data on the lymphatic drainage, obtained using different (mostly invasive) methods and in different species, diverge very widely (reviewed in ref 88). Our PET data suggest that, in the absence of invasive procedures, there is no or little such drainage in primates, and in rats there is definitely no lymphatic drainage in the spine; the cerebral lymphatic drainage in rats is apparently significant (based on the accumulation of intrathecally administered radiolabeled material in deep submandibular and/or cervical lymph nodes) and needs further investigation.

Our preliminary studies in rats with radiolabeled microspheres with calibrated diameters indicate that the functional size of the pores is at least 1  $\mu\text{m}$ , which is in agreement with the previous electron microscopy data. We have also found size dependence in the macromolecule drainage in the 2–20 nm region,<sup>49</sup> which suggests the presence of another set of either true pores or transcytosis processes functionally indistinguishable from pores (not unlike the “large endothelial pores”<sup>89</sup>).

The PET imaging data also demonstrates the immediate, without a delay, start of accumulation of the phage and protein substance leaving the LMS. The accumulation occurs in the same organs that accumulate the same materials from the systemic circulation after intravenous administration. At the same time, there is no accumulation in any lymph nodes (which avidly accumulate these materials from the interstitium). Thus, the CSF appears to drain predominantly or almost exclusively from the leptomeningeal space directly to the blood and not through consecutive transfer to the extradural interstitium and then to the lymphatics and only then to the blood.

Overall, the available data suggest that the anatomical location and distribution of pores in the LMS vary in different species very significantly. The mechanisms of both pore formation and CSF drainage through them are not known. Thus, the non-human primate model is presently the only animal model for which extrapolation of the pharmacokinetic data to humans is relatively straightforward. The continuity of the physiology of CSF drainage (and, in turn, of the data on drug behavior in CSF) between primates and other species remains to be established.

## ■ DRUG ENTRANCE FROM CSF TO CNS PARENCHYMA

The direction of the flow of the interstitial fluid from the deep regions of the brain is believed to be outward.<sup>90,91</sup> This may appear to prevent drug access from CSF to the parenchyma,

especially in large animals. However, the available data suggest that macromolecules and nanoparticles do penetrate deep into the brain, and the transfer from CSF to the brain is too fast<sup>24,26</sup> to be explained by diffusion. Hence, an active mechanism appears to participate in the parenchymal translocation of the macromolecular solutes from CSF. At this time, perivascular (perhaps mostly periarterial) transport appears to be responsible for the penetration.

**a. Perivascular Transport into the Brain.** Arteries and veins of the brain, unlike the blood vessels in other tissues, run inside liquid-filled “tubes” (Virchow–Robin spaces<sup>92,93</sup>). In spite of a large number of anatomical studies with light and electron microscopy, the exact relations of the perivascular and leptomeningeal spaces remains unclear and may vary between mammalian species.<sup>94</sup> While in some reports the continuation of the leptomeningeal sheath into the perivascular space is clearly seen, in others it is not.<sup>95–99</sup> It has been suggested that the perivascular space is connected with the lymphatic system.<sup>100</sup> Some studies suggest that there is a subpial space extending into the perivascular spaces.<sup>98,101</sup> Functional studies, however, clearly demonstrated the continuity of the leptomeningeal and perivascular spaces<sup>101–103</sup> (Figure 6).

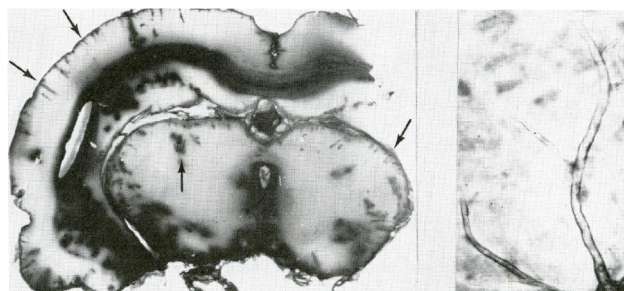


**Figure 6.** Penetration of peroxidase molecules from CSF to VRS (left) and them to parenchyma (right). Reprinted with permission from ref 103. Copyright 1974 Springer-Verlag.

Protein penetration from the CSF into the perivascular space was detected as early as at 4 min after the injection,<sup>102</sup> with spread to subpial space and with indications of back-and-forth flow.<sup>101</sup> The data, however, were qualitative, and the fraction of the solute delivered to the perivascular space was not determined. Our PET data shows that in *M. fascicularis* at 2.5 h after the injection up to ca. 10–15% of the intrathecally administered dose of proteins and phage particles can be localized in the brain volume (excluding the ventricles), and by 24 h this value decreases to 1.5–2% of the injected dose, in some animals up to 6%. The subsequent washout is slower (estimated half-life 15–20 h). This is in agreement with the entrance of the solute from CSF to the perivascular space during the first hours after the injection, when the solute concentration in the CSF is still high, followed by partial exit of the solute back to the CSF when its concentration in the latter is significantly reduced due to the CSF replacement (drainage). The residual fraction is most likely transferred to the parenchyma and taken up by the cells, and the slower process of the label (<sup>124</sup>I) washout relates to the metabolization and deiodination of the administered material. If the above is the case, the fraction of the dose remaining in the parenchyma may possibly be increased via enhancing the transport of the drug from the VRS to the parenchyma.

**b. Transport from VRS to the Brain Parenchyma.** While the data of H. Wagner et al.<sup>103</sup> and more recent studies<sup>24,104,105</sup> unequivocally demonstrate translocation of large molecules from CSF to the brain parenchyma along perivascular spaces, the mechanism(s) of their exit from the perivascular space are unknown. According to the current understanding of the structures surrounding VRS, they have to be transferred through glia limitans (formed by astrocyte endfeet) in smaller vessels and, in addition to that, through pia mater (formed by pial cells) in relatively large vessels. Only large vessels have perivascular space layered with pia;<sup>106</sup> the perivascular spaces of smaller vessels have only glial sheaths.

The properties of the pial cells lining VRS have not been studied in detail. They are possibly of the same type as meningeal cells for which the presence of endocytosis- and transcytosis-associated receptors have been demonstrated. Thus it is possible that the transfer of large molecules and particles from the VRS to the CNS parenchyma may be enhanced through chemical modification enabling receptor binding and transcytosis.

The most recent structural studies suggest that glia limitans (also known as glial limiting membrane, GLM) is formed by monolayers of astrocytic processes and/or somata irrespective of the types of blood vessel. However, the thickness of the layer decreased in the order of arterioles, venules, and capillaries.<sup>107</sup> The exact functionality of the glial layer surrounding perivascular spaces has not been studied in detail. However, the published data<sup>24,103–105,108</sup> clearly demonstrate that both pia and perivascular glia limitans are penetrable for macromolecules and particles, whether the penetration is a result of passive convective process or transcytosis. Penetration was observed around both periarterial and perivenous space.<sup>105</sup> In a study utilizing advanced in vivo imaging methods<sup>108</sup> in mice, paravenous accumulation appeared much later (>1 h after intracisternal administration) than paraarterial accumulation (immediately after the administration).

Ependymal cells lining ventricles are very different from leptomeningeal cells. They are of neuroglial origin<sup>109</sup> and have stem cell characteristics.<sup>110</sup> Thus, solute penetration to the parenchyma from the ventricles can be expected to have different kinetics and different dependence on structural and physiological factors than solute transport from VRS. They are known to express ICAM-1 and VCAM-1,<sup>144</sup> which can possibly be used for enhanced drug transport if these cells have the same CAM-associated mechanisms as the “classical” epithelial cells.<sup>111</sup>

## ■ DRUG TRANSPORT IN THE BRAIN PARENCHYMA

While the fact that macromolecules can enter the brain parenchyma through the perivascular space is well supported by experimental data, the direction(s) and rate(s) of their movement within the parenchyma are not yet fully understood. The available data suggests this process is dominated by convective transport (“bulk flow”), and the role of diffusion in the flux of the solute is much less significant. The latter was established in studies where various compounds were injected into the brain through a catheter or a needle in a small volume. Their translocation from the injection site was found to be practically independent of the molecular weight.<sup>112</sup> Infusion of therapeutic preparations through this route (“convection-enhanced delivery”<sup>113</sup>) is being actively studied clinically, predominantly in neuro-oncology.<sup>114</sup>

Investigation of the interstitial transport of various compounds injected in the brain provided valuable data on the parenchymal transport routes, including estimates for distribution volumes of the injectate (which can be determined by imaging)<sup>115</sup> and information on the directionality and reproducibility of the injectate transport, including translocation along white matter tracts<sup>116</sup> and the existence of optimal injection sites for injectate delivery to certain regions.<sup>117</sup> It was also shown that drug forms with lower tissue affinity enable wider tissue coverage than ones with higher affinity,<sup>118</sup> and that the kinetic parameters of transport may depend on anesthesia and other factors.<sup>119</sup> Although the physiology of intrathecal bolus suggests drug entrance to the parenchyma at multiple “injection points” (perivascular sites), the locations of which have not been studied in detail, the information obtained in single injection studies can be highly useful in the development and optimization of drugs intended for intrathecal delivery to CNS.

## ■ AXONAL TRANSPORT

Anterograde axonal transport of gene vectors, detected by the expression of intrathecally administered gene vectors in dorsal root ganglia, was demonstrated by Wang et al.<sup>120</sup> In our studies<sup>24</sup> with iduronate-2-sulfatase (I2S), a 6-phosphomannosylated recombinant human protein, the observed association of I2S with neurofilaments was indicative of active axonal transport. The latter likely began with protein interaction with neuronal mannose-6-phosphate receptors,<sup>121</sup> which are widely expressed on cells of the spinal cord and brain.<sup>122</sup> Thus, axonal transport is another active process that can potentially be used for enhanced (through molecule/particle modification) macromolecule and particle delivery from the leptomeningeal space to the CNS.

## ■ LEPTOMENINGEAL CELLS AND DRUG TRANSPORT

The leptomeningeal space contains several variably membranous and fibrous structures crossing the reservoir filled with CSF (Figure 1). Drug molecules and particles moving along the compartment may interact with these structures, and (if there is such interaction) their transport may be attenuated. Hypothetically, higher affinity to the leptomeningeal structures, lower dose, and slower injection/infusion should generally result in a greater “anchoring” or localization. (This is most likely the underlying mechanism of the well-localized spinal action when hydrophobic anesthetics are delivered by slow infusion from implanted pumps<sup>123</sup>). Our preliminary data showed that hydrophilic proteins, pegylated nanoparticles (up to 1.2  $\mu\text{m}$  tested), and phage particles do not bind the leptomeningeal structures and readily translocate along the compartment in all directions for several hours (see, e.g., Figure 5 in ref 25 and Figure 7 in ref 26). However, hydrophobic nanoparticles remained within 2 cm from the lumbar injection point, presumably due to nonspecific binding to the arachnoid. Thus, adhesivity of the macromolecules and particles can be used to regulate their transport in the LMS.

The meningeal structures are lined with cells of neuroectodermal origin<sup>124</sup> that have not been extensively studied. Cellular phenotypes are variable, though typically consist of elongated, spindle-shaped epithelial cells.<sup>125</sup> They express epithelial and mesothelial membrane markers, EMA/MUC1 and mesothelin,<sup>126</sup> and also cytokeratin, desmoplakin, and vimentin.<sup>125</sup> They are capable of cytochalasin B inhibitable

endocytosis<sup>127</sup> and known to express ICAM-1<sup>128</sup> and somatostatin,<sup>129</sup> but there is no information on the expression of other receptors, e.g., endocytosis-associated ones, which can play important roles in molecule/particle pharmacokinetics in CSF. Many cell surface proteins may potentially interact with the administered macromolecules and particles, thus further investigation of the meningeal cells to understand their potential role in the leptomeningeal drug delivery is warranted. The same relates to the cells lining the perivascular space (which are likely of the same type). Better understanding of the character and functions of these cells would allow targeted modification of drug molecules and particles enhancing their transport from the LMS and VRS to the parenchyma. The technological approaches for such modification are well developed.<sup>35</sup>

## ■ PATHOLOGY AND LEPTOMENINGEAL TRANSPORT

Pathological processes, such as cancer and inflammation, are known to affect the structure and function of tissues that potentially can influence leptomeningeal drug delivery.

In many pathologies, the VRS are dilated, which may result in an enhanced drug delivery to CNS parenchyma. Brain trauma results in pathologically dilated VRS.<sup>130–132</sup> Dilated VRS were also associated with migraine,<sup>133</sup> mucopolysaccharidosis,<sup>134</sup> cryptococcosis,<sup>135</sup> age,<sup>136</sup> hypertension, dementia, incidental white matter lesions,<sup>137</sup> and other conditions; the mechanism of dilation is believed to be associated with inflammatory changes, but has not been established.<sup>132</sup> The permeability of the dilated VRS walls, which may differ from the normal perivascular permeability, have not been studied.

Meningeal cancer can affect CSF movement, which can significantly alter the leptomeningeal pharmacokinetics.<sup>138</sup> Although some cranial cancers reportedly do not invade VRS,<sup>139</sup> most meningeal and brain cancers invade and/or occlude the VRS,<sup>140–143</sup> which may limit or halt drug transport. Infection-related factors can induce expression of inflammation associated receptors in the meninges<sup>128,144</sup> and potentially alter the functionality of the leptomeningeal pores, which can also attenuate drug transport. On the other hand, the inflammation induced transcytotic pathways in the VRS could enhance the transport from the VRS to the CNS parenchyma.

Thus, a variety of pathology related factors may affect the leptomeningeal transport of large molecules and particles to CNS, and the influence of these factors depends also on the character of the macromolecule/particle surface, which should be taken into account in drug development.

## ■ ADEQUACY OF ANIMAL MODELS

Interspecies variations of several physiological factors defining the intrathecal drug delivery route are very significant. Physical dimensions of the liquid compartments and the brain, intensity of the pulsatile remixing of CSF and perivascular liquid, CSF and interstitial fluid generation and turnover, and protein concentration in CSF<sup>145</sup> are different and must be taken into account in projecting animal data to humans. There is no reason to believe that mechanism-based comparative modeling cannot provide reliable data scaling, provided that quantitative data are available on all stages of transport in humans and the respective model species, of which rodents would be of highest priority in view of the availability of several developed models of disease and relatively low cost. However, until such data

become available, non-human primates will likely remain the most reliable model for pharmacokinetics studies.

## ■ CONCLUSION

The available data on the physiology of the leptomeningeal space suggests that the leptomeningeal (intrathecal) route may be useful for delivery of drugs of macromolecular and particulate nature to CNS.

The efficacy of the leptomeningeal transport is greatly affected by the volume of the intrathecal bolus. The transport is assisted by pulsation-induced turbulence in the leptomeningeal and perivascular liquid compartments. The leptomeningeal phase is followed by, hypothetically, either active or passive translocation from the VRS to the parenchyma. The latter may be followed by axonal transport.

The outcome of the leptomeningeal transport depends on the pulsatile turbulence of the leptomeningeal space, drug molecule/particle interactions with a variety of leptomeningeal and perivascular cells, and CSF drainage. These factors are not fully studied and understood, which, in view of the potential benefits of the leptomeningeal drug delivery to the CNS, warrants further studies.

## ■ AUTHOR INFORMATION

### Corresponding Author

\*E-mail: papisov@helix.mgh.harvard.edu.

### Notes

The authors declare no competing financial interest.

## ■ ACKNOWLEDGMENTS

Authors thank Drs. P. Calias, R. Penn, M. Heartlein, T. McCauley, A. J. Fischman, and R. Fisher for valuable discussions, and E. Papisov for assistance with editing the manuscript. Previously unpublished data were from studies supported by NIH Grant R21 CA152384 and DoD Grant BC100684.

## ■ ABBREVIATIONS USED

CNS, central nervous system; CSF, cerebrospinal fluid; LMS, leptomeningeal space; VRS, Virchow–Robin space; CAM, cell adhesion molecule

## ■ REFERENCES

- (1) Pardridge, W. M. The blood-brain barrier: Bottleneck in brain drug development. *NeuroRx* **2005**, 2, 3–14.
- (2) Bruni, S.; Loschi, L.; Incerti, C.; Gabrielli, O.; Coppa, G. V. Update on treatment of lysosomal storage diseases. *Acta Myol* **2007**, 26, 87–92.
- (3) Smith, M. A.; Seibel, N. L.; Altekruze, S. F.; Ries, L. A.; Melbert, D. L.; O'Leary, M.; Smith, F. O.; Reaman, G. H. Outcomes for children and adolescents with cancer: challenges for the twenty-first century. *J Clin. Oncol.* **2010**, 28, 2625–2634.
- (4) Barinaga, M. Neurotrophic factors enter the clinic. *Science* **1994**, 264, 772–774.
- (5) Zhang, Y.; Pardridge, W. M. Delivery of  $\beta$ -Galactosidase to Mouse Brain via the Blood-Brain Barrier Transferrin Receptor. *J. Pharmacol. Exp. Ther.* **2005**, 313, 1075–1081.
- (6) Cheng, S. H.; Smith, A. E. Gene therapy progress and prospects: gene therapy of lysosomal storage disorders. *Gene Ther.* **2003**, 10, 1275–1281.
- (7) Banks, W. A.; Farr, S. A.; Butt, W.; Kumar, V. B.; Franko, M. W.; Morley, J. E. Delivery across the blood-brain barrier of antisense directed against amyloid beta: reversal of learning and memory deficits

in mice overexpressing amyloid precursor protein. *J. Pharmacol. Exp. Ther.* **2001**, 297, 1113–1121.

(8) Vinogradov, S. V.; Batrakova, E. V.; Kabanov, A. V. Nanogels for oligonucleotide delivery to the brain. *Bioconjugate Chem.* **2004**, 15, 50–60.

(9) Fink, D. J.; DeLuca, N. A.; Goins, W. F.; Glorioso, J. C. Gene transfer to neurons using herpes simplex virus-based vectors. *Annu. Rev. Neurosci.* **1996**, 19, 265–287.

(10) Kaplitt, M. G.; Leone, P.; Samulski, R. J.; Xiao, X.; Pfaff, D. W.; OMalley, K.; Doring, M. J. Long-term expression and phenotypic correction using adeno-associated virus vectors in the mammalian brain. *Nat. Genet.* **1994**, 8, 148–154.

(11) Pardridge, W. M. Drug and gene delivery to the brain: the vascular route. *Neuron* **2002**, 36, 555–558.

(12) Pardridge, W. M. Biopharmaceutical drug targeting to the brain. *J. Drug Targeting* **2010**, 18, 157–167.

(13) Dickson, P. I. Delivering drugs to the central nervous system: an overview. *Drug Delivery Transl. Res.* **2012**, 2, 145–151.

(14) Muro, S. Strategies for delivery of therapeutics into the central nervous system for treatment of lysosomal storage disorders. *Drug Delivery Transl. Res.* **2012**, 2, 169–186.

(15) Vinogradov, S. V.; Bronich, T. K.; Kabanov, A. V. Nanosized cationic hydrogels for drug delivery: preparation, properties and interactions with cells. *Adv. Drug Delivery Rev.* **2002**, 54, 135–147.

(16) Wagner, H. J.; Pilgrim, C.; Brandl, J. Penetration and removal of horseradish peroxidase injected into cerebrospinal fluid. *Acta Neuropath.* **1974**, 27, 299–315.

(17) Meuli-Simmen, C.; Liu, Y.; Yeo, T. T.; Liggitt, D.; Tu, G.; Yang, T.; Meuli, M.; Knauer, S.; Heath, T. D.; Longo, F. M.; Debs, R. J. Gene expression along the cerebral-spinal axis after regional gene delivery. *Hum. Gene Ther.* **1999**, 10, 2689–2700.

(18) Shi, L.; Tang, G. P.; Gao, S. J.; Ma, Y. X.; Liu, B. H.; Li, Y.; Zeng, J. M.; Ng, Y. K.; Leong, K. W.; Wang, S. Repeated intrathecal administration of plasmid DNA complexed with polyethylene glycol-grafted polyethylenimine led to prolonged transgene expression in the spinal cord. *Gene Ther.* **2003**, 10, 1179–1188.

(19) Ishigaki, A.; Aoki, M.; Nagai, M.; Warita, H.; Kato, S.; Kato, M.; Nakamura, T.; Funakoshi, H.; Itoyama, Y. Intrathecal Delivery of Hepatocyte Growth Factor From Amyotrophic Lateral Sclerosis Onset Suppresses Disease Progression in Rat Amyotrophic Lateral Sclerosis Model. *J. Neuropathol. Exp. Neurol.* **2007**, 66, 1037–1044.

(20) Tsai, S. Y.; Markus, T. M.; Andrews, E. M.; Cheatwood, J. L.; Emerick, A. J.; Mir, A. K.; Schwab, M. E.; Kartje, G. L. Intrathecal treatment with anti-Nogo-A antibody improves functional recover in adult rats after stroke. *Exp. Brain Res.* **2007**, 182, 261–266.

(21) Kakkis, E.; McEntee, M.; Vogler, C.; Le, S.; Levy, B.; Belichenko, P.; Mobley, W.; Dickson, P.; Hanson, S.; Passage, M. Intrathecal enzyme replacement therapy reduces lysosomal storage in the brain and meninges of the canine model of MPS I. *Mol. Genet. Metab.* **2004**, 83, 163–174.

(22) Hemsley, K. M.; Hopwood, J. J. Delivery of recombinant proteins via the cerebrospinal fluid as a therapy option for neurodegenerative lysosomal storage diseases. *Int. J. Clin. Pharmacol. Ther.* **2009**, 47 (Suppl. 1), S118–S123.

(23) Milligan, E. D.; Sloane, E. M.; Langer, S. J.; Hughes, T. S.; Jekich, B. M.; Frank, M. G.; Mahoney, J. H.; Levkoff, L. H.; Maier, S. F.; Cruz, P. E.; Flotte, T. R.; Johnson, K. W.; Mahoney, M. M.; Chavez, R. A.; Leinwand, L. A.; Watkins, L. R. Repeated intrathecal injections of plasmid DNA encoding interleukin-10 produce prolonged reversal of neuropathic pain. *Pain* **2006**, 126, 294–308.

(24) Calias, P.; Papisov, M.; Pan, J.; Savioli, N.; Belov, V.; Huang, Y.; Lotterhand, J.; Alessandrini, M.; Liu, N.; Fischman, A. J.; Powell, J. L.; Heartlein, M. W. CNS Penetration of Intrathecal-Lumbar Idursulfase in the Monkey, Dog and Mouse: Implications for Neurological Outcomes of Lysosomal Storage Disorder. *PLoS ONE* **2011**, 7 (1), e30341 DOI: 10.1371/journal.pone.0030341.

(25) Papisov, M.; Belov, V.; Fischman, A. J.; Belova, E.; Titus, J.; Gagne, M.; Gillooly, C. Delivery of proteins to CNS as seen and

measured by Positron Emission Tomography. *Drug Delivery Transl. Res.* **2012**, 2, 201–209.

(26) Papisov, M.; Belov, V.; Belova, E.; Fischman, A. J.; Fisher, R.; Wright, J. L.; Gannon, K. S.; Titus, J.; Gagne, M.; Gillooly, C. A. Investigation of intrathecal transport of NPT002, a prospective therapeutic based on phage M13, in non-human primates. *Drug Delivery Transl. Res.* **2012**, 2, 210–221.

(27) Corning, J. L. Spinal anesthesia and local medication of the cord. *N.Y. Med. J.* **1885**, 42, 483–485.

(28) Koster, H.; Kasman, L. P. Spinal anaesthesia for the head, neck and thorax; its relations to respiratory paralysis. *Surg. Gynecol. Obstet.* **1929**, 49, 617–630.

(29) Yaksh, T. L.; Reddy, S. V. R. Studies in the primates on the analgetic effects associated with intrathecal actions of opiates,  $\alpha$ -adrenergic agonists and baclofen. *Anesthesiology* **1981**, 54, 451–467.

(30) Cousins, M. J.; Mather, L. E. Intrathecal and epidural administration of opioids. *Anesthesiology* **1984**, 61, 276–310.

(31) Mackey, D. C., The history of spinal drug delivery: the evolution of lumbar puncture and spinal narcosis. In *Spinal Drug Delivery*; Yaksh, T. L., Ed.; Elsevier: 1999; pp 1–41.

(32) Maythaler, J. M. Intrathecally delivered medications for spasticity and dystonia. In *Spinal Drug Delivery*; Yaksh, T. L., Ed.; Elsevier: 1999; pp 513–529.

(33) Penn, R. D.; Kroin, J. S. Continuous intrathecal baclofen for severe spasticity. *Lancet* **1985**, 326, 125–127.

(34) Di Chiro, G. Observations on the circulation of the cerebrospinal fluid. *Acta Radiol.: Diagn.* **1966**, 5, 988–1002.

(35) Soderquist, R. G.; Mahoney, M. J. Central nervous system delivery of large molecules: challenges and new frontiers for intrathecally administered therapeutics. *Expert Opin. Drug Delivery* **2010**, 7, 285–293.

(36) Dickson, P.; McEntee, M.; Vogler, C.; Le, S.; Levy, B.; Peinovich, M.; Hanson, S.; Passage, M.; Kakkis, E. Intrathecal enzyme replacement therapy: successful treatment of brain disease via the cerebrospinal fluid. *Mol. Genet. Metab.* **2007**, 91, 61–68.

(37) Xu, S.; Wang, L.; El-Banna, M.; Sohar, I.; Sleat, D. E.; Lobel, P. Large-volume Intrathecal Enzyme Delivery Increases Survival of a Mouse Model of Late Infantile Neuronal Ceroid Lipofuscinosis. *Mol. Ther.* **2011**, 19, 1842–1848.

(38) Dickson, P. I.; Ellinwood, N. M.; Brown, J. R.; Witt, R. G.; Le, S. Q.; Passage, M. B.; Vera, M. U.; Crawford, B. E. Specific antibody titer alters the effectiveness of intrathecal enzyme replacement therapy in canine mucopolysaccharidosis I. *Mol. Genet. Metab.* **2012**, 106, 68–72.

(39) Crawley, A. C.; Marshall, N.; Beard, H.; Hassiotis, S.; Walsh, V.; King, B.; Hucker, N.; Fuller, M.; Jolly, R. D.; Hopwood, J. J.; Hemsley, K. M. Enzyme replacement reduces neuropathology in MPS IIIA dogs. *Neurobiol. Dis.* **2011**, 43, 422–434.

(40) Okuda, Y.; Sakoda, S.; Fujimura, H.; Nagata, S.; Yanagihara, T.; Bernard, C. C. Intrathecal administration of neutralizing antibody against Fas ligand suppresses the progression of experimental autoimmune encephalomyelitis. *Biochem. Biophys. Res. Commun.* **2000**, 275, 164–168.

(41) Cahill, C. M.; Dray, A.; Coderre, T. J. Intrathecal nerve growth factor restores opioid effectiveness in an animal model of neuropathic pain. *Neuropharmacology* **2003**, 45, 543–552.

(42) Bambakidis, N. C.; Petrullis, M.; Kui, X.; Rothstein, B.; Karampela, I.; Kuang, Y.; Selman, W. R.; LaManna, J. C.; Miller, R. H. Improvement of neurological recovery and stimulation of neural progenitor cell proliferation by intrathecal administration of Sonic hedgehog. *J. Neurosurg.* **2012**, 116, 1114–1120.

(43) Im, Y. B.; Jee, M. K.; Choi, J. I.; Cho, H. T.; Kwon, O. H.; Kang, S. K. Molecular targeting of NOX4 for neuropathic pain after traumatic injury of the spinal cord. *Cell Death Dis.* **2012**, 3, e426. doi: 10.1038/cddis.2012.168.

(44) Vanderah, T. W.; Laughlin, T.; Lashbrook, J. M.; Nichols, M. L.; Wilcox, G. L.; Ossipov, M. H.; Malan, T. P., Jr; Porreca, F. Single intrathecal injections of dynorphin A or des-Tyr-dynorphins produce long-lasting allodynia in rats: blockade by MK-801 but not naloxone. *Pain* **1996**, 68, 275–281.

- (45) Ochs, G.; Penn, R. D.; York, M.; Giess, R.; Beck, M.; Tonn, J.; Haigh, J.; Malta, E.; Traub, M.; Sendtner, M.; Toyka, K. V. A phase I/II trial of recombinant methionyl human brain derived neurotrophic factor administered by intrathecal infusion to patients with amyotrophic lateral sclerosis. *Amyotrophic Lateral Scler. Other Mot. Neuron Disord.* **2000**, *1*, 201–206.
- (46) Nauta, H. J. W.; Dolan, E.; Yasaargil, M. G. Microsurgical anatomy of spinal subarachnoid space. *Surg. Neurol.* **1983**, *19*, 431–437.
- (47) Riesebach, R.; DiChiro, G.; Freireich, E. J.; Rall, D. P. Subarachnoid distribution of drugs after lumbar injection. *New Engl. J. Med.* **1962**, *267*, 1273–1278.
- (48) Lu, J.; Zhu, X. L. Cranial arachnoid membranes: some aspects of microsurgical anatomy. *Clin. Anat.* **2007**, *20*, S02–S11.
- (49) Belova, E.; Papisov, M.; et al. 2012, unpublished data.
- (50) Barker, A. E. A report on clinical experiences with spinal analgesia in 100 cases, and some reflections on the procedure. *Br. Med. J.* **1907**, *1*, 665–674.
- (51) Kirshner, M. Spinal zone anesthesia. Placed at will and dosage individually graded. *Surg. Gynecol. Obstet.* **1932**, *55*, 317–329.
- (52) Brown, D. T.; Wildsmith, J. A.; Covino, B. G.; Scott, D. B. Effect of baricity on spinal anaesthesia with amethocaine. *Br. J. Anaesth.* **1980**, *52*, 589–596.
- (53) Stienstra, R.; Gielen, M.; Kroon, J. W.; Van Poorten, F. The influence of temperature and speed of injection on the distribution of a solution containing bupivacaine and methylene blue in a spinal canal model. *Reg. Anesth.* **1990**, *15*, 6–11.
- (54) Davson, H.; Segal, M. B. *Physiology of the CSF and Blood-brain barriers*; CRC: Boca Raton, 1995.
- (55) Zheng, W.; Chodobski, A., Eds. *The blood-cerebrospinal fluid barrier*; Chapman & Hall/CRC: Boca Raton, 2005.
- (56) Oldendorf, W. H.; Davson, H. Brain extracellular space and the sink action of the cerebrospinal fluid. Measurement of rabbit brain extracellular space using sucrose labeled with carbon 14. *Arch. Neurol.* **1967**, *17*, 196–205.
- (57) Kimelberg, H. K. Water homeostasis in the brain: basic concepts. *Nat. Neurosci.* **2004**, *129*, 851–860.
- (58) O'Connell, J. E. A. Vascular factor in intracranial pressure and maintenance of cerebrospinal fluid circulation. *Brain* **1943**, *66*, 204–228.
- (59) Oreskovic, D.; Klarica, M. Development of hydrocephalus and classical hypothesis of cerebrospinal fluid hydrodynamics: facts and illusions. *Prog. Neurobiol.* **2011**, *94*, 238–258.
- (60) Dandy, W. E.; Blackfan, K. D. Internal hydrocephalus. An experimental, clinical and pathological study. *Am. J. Dis. Child.* **1914**, *8*, 406–482.
- (61) Ingraham, F. D.; Matson, D. D.; Alexander, E.; Woods, P. P. Studies in the treatment of experimental hydrocephalus. *J. Neuropathol. Exp. Neurol.* **1948**, *7*, 123–143.
- (62) Sachs, E.; Wilkins, H.; Sams, C. F. Studies on cerebrospinal circulation by a new method. *Arch. Neurol. Psychiatry* **1930**, *23*, 130–151.
- (63) Di Chiro, G.; Hammock, M. K.; Bleyer, W. A. Spinal descent of cerebrospinal fluid in man. *Neurology* **1976**, *26*, 1–8.
- (64) Reid, A.; Marchbanks, R. J.; Ernst, A. *Intracranial and Inner Ear Physiology and Pathophysiology*; Whurr Publishers: London, 1998; p 9.
- (65) Enzmann, D. R.; Pelc, N. J. Normal flow patterns of intracranial and spinal cerebrospinal fluid defined with phase-contrast cine MR imaging. *Radiology* **1991**, *178*, 467–474.
- (66) Yoshida, K.; Takahashi, H.; Saijo, M.; Ueguchi, T.; Tanaka, H.; Fujita, N.; Murase, K. Phase-contrast MR studies of CSF flow rate in the cerebral aqueduct and cervical subarachnoid space with correlation-based segmentation. *Magn. Reson. Med. Sci.* **2009**, *8*, 91–100.
- (67) Henry-Feugeas, M. C. Temporal and spatial assessment of normal cerebrospinal fluid dynamics with MR imaging. *Magn. Reson. Imaging* **1993**, *11*, 1107–1118.
- (68) Zhu, D. C.; Xenos, M.; Linninger, A. A.; Penn, R. D. Dynamics of lateral ventricle and cerebrospinal fluid in normal and hydrocephalic brains. *J. Magn. Reson. Imaging* **2006**, *24*, 756–770.
- (69) Bhadelia, R. A.; Bogdan, A. R.; Kaplan, R. F.; Wolpert, S. M. Cerebrospinal fluid pulsation amplitude and its quantitative relationship to cerebral blood flow pulsations: a phase-contrast MR flow imaging study. *Neuroradiology* **1997**, *39*, 258–264.
- (70) Linge, S. O.; Haughton, V.; Løvgren, A. E.; Mardal, K. A.; Langtangen, H. P. CSF flow dynamics at the craniovertebral junction studied with an idealized model of the subarachnoid space and computational flow analysis. *Am. J. Neuroradiol.* **2010**, *31*, 185–192.
- (71) Sweetman, B.; Linninger, A. A. Cerebrospinal fluid flow dynamics in the central nervous system. *Ann. Biomed. Eng.* **2011**, *39*, 484–496.
- (72) Loth, F.; Yardimci, A. M.; Alperin, N. Hydrodynamic modeling of cerebrospinal fluid motion within the spinal cavity. *J. Biomech. Eng.* **2001**, *123*, 71–79.
- (73) Linninger, A. A.; Xenos, M.; Sweetman, B.; Ponskshe, S.; Guo, X.; Penn, R. A mathematical model of blood, cerebrospinal fluid and brain dynamics. *J. Math. Biol.* **2009**, *59*, 729–759.
- (74) Du Boulay, G. H.; O'Connell, J.; Currie, J.; Bostick, T.; Verity, P. Further investigation of pulsatile movements in the cerebrospinal fluid pathways. *Acta Radiol.: Diagn.* **1972**, *13*, 496–523.
- (75) Hettiarachchi, H. D.; Hsu, Y.; Harris, T. J., Jr; Penn, R.; Linninger, A. A. The effect of pulsatile flow on intrathecal drug delivery in the spinal canal. *Ann. Biomed. Eng.* **2011**, *39*, 2592–2602; Erratum in *Ann. Biomed. Eng.* **2011**, *39*, 2603.
- (76) Davson, H.; Segal, M. B. *Physiology of the CSF and Blood-Brain Barriers*; CRC: Boca Raton, 1995; p 201.
- (77) Kapoor, K. G.; Katz, S. E.; Grzybowski, D. M.; Lubow, M. Cerebrospinal fluid outflow: an evolving perspective. *Brain Res. Bull.* **2008**, *77*, 327–334.
- (78) Levine, J. E.; Povlishock, J. T.; Becker, D. P. The Morphological Correlates of Primate Cerebrospinal Fluid Absorption. *Brain Res.* **1982**, *241*, 31–41.
- (79) Weed, L. H. The absorption of cerebrospinal fluid into the venous system. *Am. J. Anat.* **1923**, *31*, 191–221.
- (80) Maurizi, C. P. Arachnoid granules: Dandy was Dandy, Cushing and Weed were not. *Med. Hypotheses* **2010**, *75*, 238–240.
- (81) Welch, K.; Friedman, V. The cerebrospinal fluid valves. *Brain* **1960**, *83*, 454–469.
- (82) Welch, K.; Pollay, M. The spinal arachnoid villi of the monkeys *Cercopithecus aethiops* and *Macaca irus*. *Anat. Rec.* **1963**, *145*, 43–48.
- (83) McComb, J. G.; Davson, H.; Hollingsworth, J. R. Attempted separation of blood-brain and blood-cerebrospinal fluid barriers in the rabbit. *Exp. Eye Res.* **1977**, *25*, 333–343.
- (84) Butler, A.; Mann, J.; Bass, N. Identification of the major site for cerebrospinal fluid efflux in the albino rat. *Anat. Rec.* **1975**, *181*, 323.
- (85) Tripathi, R. Tracing the bulk outflow route of cerebrospinal fluid by transmission and scanning electron microscopy. *Brain Res.* **1974**, *503*, 503–506.
- (86) Butler, A. B.; Mann, J. D.; Bass, N. H. Vesicular transport of peroxidase across the endothelium of the rat arachnoid villus. *Anat. Rec.* **1977**, *187*, 543.
- (87) Yamada, S.; DePasquale, M.; Patlak, C. S.; Cserr, H. F. Albumin outflow into deep cervical lymph from different regions of rabbit brain. *Am. J. Physiol.* **1991**, *261* (4 Part 2), H1197–H204.
- (88) Koh, L.; Zakharov, A.; Johnston, M. Integration of the subarachnoid space and lymphatics: Is it time to embrace a new concept of cerebrospinal fluid absorption? *Cerebrospinal Fluid Res.* **2005**, *2*, 6.
- (89) Michel, C. C. Transport of macromolecules through microvascular walls. *Cardiovasc. Res.* **1996**, *32*, 644–653.
- (90) Cserr, H. F.; Cooper, D. N.; Milhorat, T. H. Flow of cerebral interstitial fluid as indicated by the removal of extracellular markers from rat caudate nucleus. *Exp. Eye Res.* **1977**, *25* (Suppl.), 461–473.
- (91) Cserr, H. F.; Ostrach, L. H. Bulk flow of interstitial fluid after intracranial injection of blue dextran 2000. *Exp. Neurol.* **1974**, *45*, 50–60.

- (92) Virchow, R. Ueber die Erweiterung kleinerer Gefaesse. *Arch. Pathol. Anat. Physiol. Klin. Med.* **1851**, 3, 427–462.
- (93) Robin, C. Recherches sur quelques particularités de la structure des capillaires de l'encephale. *J. Physiol. Homme Anim.* **1859**, 2, 537–548.
- (94) Davson, H. Segal, M. B. *Physiology of the CSF and Blood-brain barriers*; CRC: Boca Raton, 1995; p 507.
- (95) Woollam, D. H. M.; Millen, J. W. The perivascular spaces of the mammalian central nervous system. *Biol. Rev.* **1954**, 29, 251–283.
- (96) Millen, J. W.; Woollam, D. H. On the nature of the pia mater. *Brain* **1961**, 84, 514–520.
- (97) Hutchings, M.; Weller, R. O. Anatomical relationships of the pia mater to cerebral blood vessels in man. *J. Neurosurg.* **1986**, 65, 316–325.
- (98) Zhang, E. T.; Inman, C. B.; Weller, R. O. Interrelationship of the pia mater and the perivascular (Virchow-Robin) spaces in the human cerebrum. *J. Anat.* **1990**, 170, 111–123.
- (99) Pollock, H.; Hutchings, M.; Weller, R. O.; Zhang, E. T. Perivascular spaces in the basal ganglia of the human brain: their relationship to lacunes. *J. Anat.* **1997**, 191, 337–346.
- (100) Schley, D.; Carare-Nnadi, R.; Please, C. P.; Perry, V. H.; Weller, R. O. Mechanisms to explain the reverse perivascular transport of solutes out of the brain. *J. Theor. Biol.* **2006**, 238, 962–974.
- (101) Ichimura, T.; Fraser, P. A.; Cserr, H. F. Distribution of extracellular tracers in perivascular spaces of the rat brain. *Brain Res.* **1991**, 545, 103–113.
- (102) Rennels, M. L.; Gregory, T. F.; Blaumanis, O. R.; Fujimoto, K.; Grady, P. A. Evidence for a paravascular fluid circulation in the mammalian central nervous system, provided by rapid distribution of tracer protein throughout the brain from subarachnoid spaces. *Brain Res.* **1985**, 326, 47–63.
- (103) Wagner, H.-J.; Pilgrim, C.; Brandl, J. Penetration and removal of horseradish peroxidase injected into cerebrospinal fluid: Role of cerebral perivascular spaces, endothelium and microglia. *Acta Neuropathol.* **1974**, 27, 299–315.
- (104) Crawley, A. C.; Marshall, N.; Beard, H.; Hassiotis, S.; Walsh, V.; King, B.; Hucker, N.; Fuller, M.; Jolly, R. D.; Hopwood, J. J.; Hemsley, K. M. Enzyme replacement reduces neuropathology in MPS IIIA dogs. *Neurobiol. Dis.* **2011**, 43, 422–434.
- (105) Jolly, R. D.; Marshall, N. R.; Perrott, M. R.; Dittmer, K. E.; Hemsley, K. M.; Beard, H. Intracisternal enzyme replacement therapy in lysosomal storage diseases: routes of absorption into brain. *Neuropathol. Appl. Neurobiol.* **2011**, 37, 414–422.
- (106) Hager, H. Elektronenmikroskopische Untersuchungen über die Feinstruktur der Blutgefäße und perivascular Räume im Säugetiergehirn. *Acta Neuropathol.* **1961**, 1, 9–33.
- (107) Watanabe, K.; Takeishi, H.; Hayakawa, T.; Sasaki, H. Three-dimensional organization of the perivascular glial limiting membrane and its relationship with the vasculature: a scanning electron microscope study. *Okajimas Folia Anat. Jpn.* **2010**, 87, 109–121.
- (108) Iliff, J. J.; Wang, M.; Liao, Y.; Plogg, B. A.; Peng, W.; Gundersen, G. A.; Benveniste, H.; Vates, G. E.; Deane, R.; Goldman, S. A.; Nagelhus, E. A.; Nedergaard, M. A Paravascular Pathway Facilitates CSF Flow Through the Brain Parenchyma and the Clearance of Interstitial Solutes, Including Amyloid  $\beta$ . *Sci. Transl. Med.* **2012**, 4, 147ra111.
- (109) Gotz, M.; Huttner, W. B. The cell biology of neurogenesis. *Nat. Rev. Mol. Cell Biol.* **2005**, 6, 777–788.
- (110) Carlén, M.; Meletis, K.; Göritz, C.; Darsalia, V.; Evergren, E.; Tanigaki, K.; Amendola, M.; Barnabé-Heider, F.; Yeung, M. S.; Nalini, L.; Honjo, T.; Kokaia, Z.; Shupliakov, O.; Cassidy, R. M.; Lindvall, O.; Frisén, J. Forebrain ependymal cells are Notch-dependent and generate neuroblasts and astrocytes after stroke. *Nat. Neurosci.* **2009**, 12, 259–267.
- (111) Ghaffarian, R.; Bhowmick, T.; Muro, S. Transport of nanocarriers across gastrointestinal epithelial cells by a new trans-cellular route induced by targeting ICAM-1. *J. Controlled Release* **2012**, 163, 25–33.
- (112) Cserr, H. F.; Cooper, D. N.; Suri, P. K.; Patlak, C. S. Efflux of radiolabeled polyethylene glycols and albumin from rat brain. *Am. J. Physiol.* **1981**, 240, F319–F328.
- (113) Bobo, R. H.; Laske, D. W.; Akbasak, A.; Morrison, P. F.; Dedrick, R. L.; Oldfield, E. H. Convection-enhanced delivery of macromolecules in the brain. *Proc. Natl. Acad. Sci. U.S.A.* **1994**, 91, 2076–2080.
- (114) Bidros, D. S.; Vogelbaum, M. A. Novel drug delivery strategies in neuro-oncology. *Neurotherapeutics* **2009**, 6, 539–546.
- (115) Iyer, R. R.; Butman, J. A.; Walbridge, S.; Gai, N. D.; Heiss, J. D.; Lonser, R. R. Tracking accuracy of T2- and diffusion-weighted magnetic resonance imaging for infusate distribution by convection-enhanced delivery. *J. Neurosurg.* **2011**, 115, 474–480.
- (116) Geer, C. P.; Grossman, S. A. Interstitial fluid flow along white matter tracts: A potentially important mechanism for the dissemination of primary brain tumors. *J. Neuro-Oncol.* **1997**, 32, 193–201.
- (117) Yin, D.; Valles, F. E.; Fiandaca, M. S.; Bringas, J.; Gimenez, F.; Berger, M. S.; Forsayeth, J.; Bankiewicz, K. S. Optimal region of the putamen for image-guided convection-enhanced delivery of therapeutics in human and non-human primates. *Neuroimage* **2011**, 54 (Suppl.1), S196–S203.
- (118) Inoue, T.; Yamashita, Y.; Nishihara, M.; Sugiyama, S.; Sonoda, Y.; Kumabe, T.; Yokoyama, M.; Tominaga, T. Therapeutic efficacy of a polymeric micellar doxorubicin infused by convection-enhanced delivery against intracranial 9L brain tumor models. *Neuro Oncol.* **2009**, 11, 151–157.
- (119) Groothuis, D. R.; Vavra, M. W.; Schlageter, K. E.; Kang, E. W.; Itskovich, A. C.; Hertzler, S.; Allen, C. V.; Lipton, H. L. Efflux of drugs and solutes from brain: the interactive roles of diffusional transcapillary transport, bulk flow and capillary transporters. *J. Cereb. Blood Flow Metab.* **2007**, 27, 43–56.
- (120) Wang, X.; Wang, C.; Zeng, J.; Xu, X.; Hwang, P.; Yee, W.-C.; Ng, Y.-K.; Wang, Sh. Gene Transfer to Dorsal Root Ganglia by Intrathecal Injection: Effects on Regeneration of Peripheral Nerves. *Mol. Ther.* **2005**, 12, 314–320.
- (121) Kar, S.; Poirier, J.; Guevara, J.; Dea, D.; Hawkes, C.; Robitaille, Y.; Quirion, R. Cellular distribution of insulin-like growth factor-II/ mannose-6-phosphate receptor in normal human brain and its alteration in Alzheimer's disease pathology. *Neurobiol. Aging* **2006**, 27, 199–210.
- (122) Hawkes, C.; Kar, S. Insulin-like growth factor-II/Mannose-6-phosphate receptor in the spinal cord and dorsal root ganglia of the adult rat. *Eur. J. Neurosci.* **2002**, 15, 33–39.
- (123) Yaksh, T. L.; Horais, K.; Tozier, N.; Allen, J.; Rathbun, M. L.; Rossi, S.; Sommer, C.; Meschter, C.; Richter, P. J.; Hildebrand, K. R. Chronically Infused Intrathecal Morphine in Dogs. *Anesthesiology* **2003**, 99, 174–187.
- (124) O'Rahilly, R.; Muller, F. The Meninges in Human Development. *J. Neuropathol. Exp. Neurol.* **1986**, 45, 588–608.
- (125) Janson, C.; Romanova, L.; Hansen, E.; Hubel, A.; Lam, C. Immortalization and functional characterization of rat arachnoid cell lines. *Neuroscience* **2011**, 177, 23–34.
- (126) Petricevic, J.; Forempoher, G.; Ostojic, L.; Mardesic-Brakus, S.; Andjelinovic, S.; Vukojevic, K.; Saraga-Babic, M. Expression of nestin, mesothelin and epithelial membrane antigen (EMA) in developing and adult human meninges and meningiomas. *Acta Histochem.* **2011**, 113, 703–711.
- (127) Feurer, D. J.; Weller, R. O. Barrier functions of the leptomeninges: a study of normal meninges and meningiomas in tissue culture. *Neuropathol. Appl. Neurobiol.* **1991**, 17, 391–405.
- (128) Endo, H.; Sasaki, K.; Tonosaki, A.; Kayama, T. Three-dimensional and ultrastructural ICAM-1 distribution in the choroid plexus, arachnoid membrane and dural sinus of inflammatory rats induced by LPS injection in the lateral ventricles. *Brain Res.* **1998**, 793, 297–301.
- (129) Feindt, J.; Krisch, B.; Lucius, R.; Mentlein, R. Meningeal cells are targets and inactivation sites for the neuropeptide somatostatin. *Brain Res. Mol. Brain Res.* **1997**, 44, 293–300.

- (130) Esiri, M. M.; Gay, D. Immunological and neuropathological significance of the Virchow-Robin space. *J. Neurol. Sci.* **1990**, *100*, 3–8.
- (131) Inglese, M.; Bomsztyk, E.; Gonen, O.; Mannon, L. J.; Grossman, R. I.; Rusinek, H. Dilated Perivascular Spaces: Hallmarks of Mild Traumatic Brain Injury. *Am. J. Neuroradiol.* **2005**, *26*, 719–724.
- (132) Inglese, M.; Grossman, R. I.; Diller, L.; Babb, J. S.; Gonen, O.; Silver, J. M.; Rusinek, H. Clinical significance of dilated Virchow-Robin spaces in mild traumatic brain injury. *Brain Inj.* **2006**, *20*, 15–21.
- (133) Schick, S.; Gahleitner, A.; Wöber-Bingöl, C.; Wöber, C.; Ba-Salamah, A.; Schoder, M.; Schindler, E.; Prayer, D. Virchow-Robin spaces in childhood migraine. *Neuroradiology* **1999**, *41*, 283–287.
- (134) Murata, R.; Nakajima, S.; Tanaka, A.; Miyagi, N.; Matsuoka, O.; Kogame, S.; Inoue, Y. MR imaging of the brain in patients with mucopolysaccharidosis. *Am. J. Neuroradiol.* **1989**, *10*, 1165–1170.
- (135) Miskiel, K. A.; Hall-Craggs, M. A.; Miller, R. F.; Kendall, B. E.; Wilkinson, I. D.; Paley, M. N.; Harrison, M. J. The spectrum of MRI findings in CNS cryptococcosis in AIDS. *Clin. Radiol.* **1996**, *51*, 842–850.
- (136) MacLullich, A. M. J.; Wardlaw, J. M.; Ferguson, K. J.; Starr, J. M.; Seckl, J. R.; Deary, I. J. Enlarged perivascular spaces are associated with cognitive function in healthy elderly men. *J. Neurol. Neurosurg. Psychiatry* **2004**, *75*, 1519–1523.
- (137) Heier, L. A.; Bauer, C. J.; Schwartz, L.; Zimmerman, R. D.; Morgello, S.; Deck, M. D. Large Virchow-Robin spaces: MR-clinical correlation. *Am. J. Neuroradiol.* **1989**, *10*, 929–936.
- (138) Mason, W. P.; Yeh, S.; DeAngelis, L. M. 111Indium-diethylenetriamine pentaacetic acid cerebrospinal fluid flow studies predict distribution of intrathecally administered chemotherapy and outcome in patients with leptomeningeal metastases. *Neurology* **1998**, *50*, 438–444.
- (139) Hassin, G. B. Histopathology of carcinoma of the cerebral meninges. *Arch. Neurol. Psychiatry* **1919**, *1*, 705–716.
- (140) Mammoser, A. G.; Groves, M. D. Biology and therapy of neoplastic meningitis. *Curr. Oncol. Rep.* **2010**, *12*, 41–49.
- (141) Mirfakhraee, M.; Crofford, M. J.; Guinto, F. C., Jr.; Nauta, H. J.; Weedn, V. W. Virchow-Robin space: a path of spread in neurosarcoidosis. *Radiology* **1986**, *158*, 715–720.
- (142) Kooistra, K. L.; Rodriguez, M.; Powis, G.; Yaksh, T. L.; Harty, G. J.; Hilton, J. F.; Laws, E. R., Jr. Development of experimental models for meningeal neoplasia using intrathecal injection of 9L gliosarcoma and Walker 256 carcinosarcoma in the rat. *Cancer Res.* **1986**, *46*, 317–323.
- (143) Herman, C.; Kupsky, W. J.; Rogers, L.; Duman, R.; Moore, P. Leptomeningeal Dissemination of Malignant Glioma Simulating Cerebral Vasculitis. *Stroke* **1995**, *26*, 2366–2370.
- (144) Deckert-Schluter, M.; Schluter, D.; Hof, H.; Wiestler, O. D.; Lassmann, H. Differential expression of ICAM-1, VCAM-1 and their ligands LFA-1, Mac-1, CD43, VLA-4 and MHC class II antigens in murine toxoplasma encephalitis: A light microscopic and ultra-structural immunohistochemical study. *J. Neuropathol. Exp. Neurol.* **1994**, *53*, 457–468.
- (145) Maurer, M. H. Proteomics of brain extracellular fluid (ECF) and cerebrospinal fluid (CSF). *Mass Spectrom. Rev.* **2010**, *29*, 17–28.

# Delivery of enzyme replacement therapeutics to CNS in rats and monkeys as seen and measured by PET

M.I. Papisov,<sup>1-3</sup> V. Belov,<sup>1-3</sup> A.J. Fischman,<sup>2,3</sup> J. Titus,<sup>1</sup> M. Gagne,<sup>1</sup> P. Calias,<sup>4</sup> T. McCauley,<sup>4</sup> M. Heartlein<sup>4</sup>

<sup>1</sup>Massachusetts General Hospital, Boston, MA; <sup>2</sup>Harvard Medical School, Boston, MA; <sup>3</sup>Shriners Hospitals for Children-Boston, Boston, MA; <sup>4</sup>Shire HGT, Cambridge, MA,  
papisov@helix.mgh.harvard.edu

## ABSTRACT SUMMARY

Hunter Syndrome, Metachromatic Leukodystrophy and Sanfilippo Syndrome are genetic lysosomal storage diseases (LSD) characterized by CNS degeneration as well as somatic symptoms. Presently, there are no effective treatments to alleviate the neurological component of these diseases. The objective of these studies was to investigate the pharmacokinetics of enzyme replacement therapeutics after intrathecal (IT) administration. The studies were also intended to evaluate the relevance of rodent models as compared with primate models and to develop methodology for fully quantitative non-invasive pharmacokinetics studies by Positron Emission Tomography (PET).

## INTRODUCTION

Leptomeningeal transfer of intrathecally administered drugs to the CNS includes convectional transport in the cerebrospinal fluid (CSF) with subsequent penetration into the brain parenchyma and spinal cord. Concurrently, a fraction of the drug drains with CSF outside of leptomeningeal space (LMS) and yet another fraction may be accumulated in the leptomeningeal cells.

Thus, the intrathecal route to CNS relies on the processes depending on insufficiently studied factors, such as remixing of CSF by the pulsatile movement of CNS tissues, drainage of CSF (presumably to the blood through mesothelial pores and to the lymphatics via paraneural interstitium), and intraparenchymal non-interstitial transfer. Investigation of complex combinations of transfer processes benefits from methods enabling: (i) whole-body quantitative registration of all transfer processes on all time frames, and (ii) real-time data acquisition in the same animal and using any animal as its own control, which removes the individual variances from the kinetic data.

PET, as a powerful tool for quantitative in-vivo imaging of the transport of pharmaceuticals labeled with positron-emitting radionuclides, meets the above requirements. With the growing number of drugs and drug delivery systems that have non-trivial pharmacokinetics PET imaging will play an increasingly significant role in preclinical (especially, non-human primate) and, possibly, human studies.

Imaging of slow PK that is characteristic for many "large molecule" drugs and drug delivery systems requires positron emitting labels (radionuclides) with long physical half-lives. Among positron emitters available

and suitable for PET, <sup>124</sup>I has the longest physical half-life of 4.2 days. This, combined with the well-investigated iodine behavior in vivo, makes <sup>124</sup>I attractive for long-term (several days) imaging studies. The decay scheme of <sup>124</sup>I is complex; its emission spectrum includes high energy positrons (23%) and high energy single photons (60.5% at 603 keV). Both the high energy of the positrons and the presence of single photons in the range close to the 511 keV of annihilation photon pairs may lead to degradation of sensitivity, spatial resolution and image quality. However, we have shown in our previous studies [1] that proper use of <sup>124</sup>I provides fully quantitative data suitable for pharmacological research.

The present studies were intended to investigate the pharmacokinetics of human recombinant enzymes after intrathecal (IT) administration in rats and non-human primates, to evaluate the relevance of rodent models vs. primate models, and develop methodology for fully quantitative non-invasive pharmacokinetics studies by Positron Emission Tomography (PET) with <sup>124</sup>I.

## EXPERIMENTAL METHODS

Three human recombinant enzymes, idursulfase, arylsulfatase A, and sulfamidase, were labeled with <sup>124</sup>I and administered at various doses, via intravenous and intrathecal routes, in rats and (the former two proteins) in cynomolgus monkeys.

Imaging was carried out using either MicroPET P4 primate PET scanner (concorde Microsystems/Siemens) or a custom PET/CT imaging system consisting of MicroPET Focus 220 PET scanner and CereTom CT scanner (Neurologica, MA).



Figure 1. Scheme of the non-human primate experiment (PET/CT image). Proteins were administered through a subcutaneous port (center) connected through a subcutaneous catheter with the leptomeningeal space. Color represents 3-dimensional map of the protein concentration as measured by PET (shown: 3 hours after the injection).

The general scheme of the non-human primate experiments is shown in Figure 1. Proteins were administered through a subcutaneous port connected through a subcutaneous catheter with the leptomeningeal space. Color represents protein concentration as measured by PET (shown: 3 hours after the injection).

In rats, intrathecal administration was carried out either via direct injection to cisterna magna through the Atlanto-Occipital joint, or through a surgically installed lumbar catheter.

Dynamic imaging data (0-20 min post injection) and multiple static images were acquired over up to 8 days after the injections. Acquisition, histogramming, and reconstruction were executed with the aid of Siemens software. CT images were used for attenuation correction and (as in Figure 1) for anatomical referencing. The numerical data from manually selected regions of interest were processed to determine the principal PK parameters.

FITC labeled sulfamidase was utilized to investigate by photoimaging the microdistribution of the protein delivered to the brain in rats [2].

## RESULTS AND DISCUSSION

Overall, our data demonstrate that leptomeningeal (intrathecal) route is suitable for protein delivery to the brain parenchyma, including both grey and white matter. Biologically significant levels of the studied proteins were found in all brain compartments at doses found in other studies to be safe [3].

The data demonstrate that the initial transfer of intrathecally administered proteins significantly depends on the injection (and port flush) volume. The literature data suggests that administration of volumes up to 30% of the total estimated CSF volume is safe for primates, both human and non-human. According to our data, lumbar protein administration with 0.5 ml/kg body weight port flush (monkeys), which is <20% of the estimated CSF volume, results in the immediate transfer of ca. 50% of the injected dose to cerebral CSF. Lumbar administration in smaller volumes results in a slower protein transfer to the cerebral CSF (Figure 2). In both cases, the protein subsequently enters brain parenchyma. Protein penetration into the brain was quantified from the imaging data and the kinetics of it was found to be in agreement with CSF replacement rate. Thus, the rate of protein transfer was maximal during the first 2-5 hours; by this time a significant (30-50%, depending on the protein) fraction was cleared from CSF to the systemic circulation.

In rats, large volume (0.05 ml CSF withdrawal followed by 0.1 ml injection) IT administration to cisterna magna resulted in rapid protein distribution over the entire CSF volume, including distal spine. The initial label content in the brain was 0.20%, 0.15% and 0.05% of injected dose/g after IV and 45%, 70% and 35% after IT administration for Idursulfase, arylsulfatase A, and sulfamidase, respectively. Idursulfase was cleared from both the brain and spinal cord with a half-life of ~7h, while for the other two enzymes the half-life was ~24 h. Photoimaging studies indicated enzyme deposition in pia mater as well as in the brain parenchyma.

PET also provided a variety of visual “4-D” data (“pharmacokinetics movies”) valuable for the initial analysis of the data, and a variety of data on protein transfer (e.g., along nerves and into lymphatics) that would not be accessible through other experimental methods.

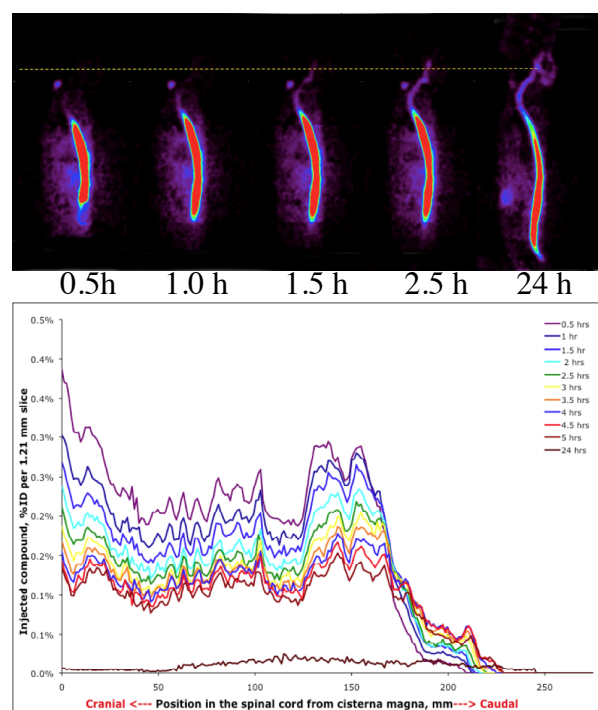


Figure 1. Top: visual representation of PET data on protein spread from the lumbar injection point in a monkey (color represents concentration). Bottom: numerical graphic representation of the same data (% of ID per unit of spine length as a function of time).

## CONCLUSIONS

The data suggest that leptomeningeal (intrathecal) route of administration can be beneficial for the treatment of CNS with biopharmaceuticals.

Several mechanistic aspects of leptomeningeal drug transport, such as parenchymal transfer, CSF drainage and mesothelial uptake, are important for understanding of the data, which warrants further investigation.

## REFERENCES

1. Belov V.V.; Bonab A.A.; Fischman A.J.; Heartlein M.; Calias P. and Papisov M.I. *Molecular Pharmaceutics* **2011**, 8, (3), 736–747.
2. M. Papisov, V. Belov, A. J. Fischman, A. A. Bonab, M. Wiles, H. Xie, M. Heartlein, P. Calias. Annual meeting of SNM, Toronto, CA, June 2009
3. Calias P.; Papisov M.; Pan J.; Savioli N.; Belov V. et al. *PLoS ONE* 2012, 7, (1), e30341-1-13.

## ACKNOWLEDGEMENTS

This work was supported by NIH grant R21 CA152384, DoD grant BC100684, and grants from Shire HGT.

# PET-based approaches to studying the size-dependence of leptomeningeal drug clearance

Elena Belova,<sup>1,3</sup> Lloyd Vallance,<sup>2,4</sup> Vasily Belov,<sup>1,3</sup> Matthew Gagne,<sup>1</sup> Caitlin Gillooly<sup>1</sup> and Mikhail Papisov<sup>1,3</sup>

<sup>1</sup>Massachusetts General Hospital, Boston, MA 02114; <sup>2</sup>Harvard University, Cambridge, MA 02138, <sup>3</sup>Shriners Hospitals for Children–Boston, Boston, MA 02114; and <sup>4</sup>Shire HGT, Lexington, MA 02421  
[belova@pet.mgh.harvard.edu](mailto:belova@pet.mgh.harvard.edu)

## ABSTRACT SUMMARY

Leptomeningeal space (LMS) provides a promising avenue for delivery of macro- and supramolecular drugs to central nervous system (CNS).<sup>1</sup> Leptomeningeal pharmacokinetics significantly depends on the turnover of the cerebrospinal fluid (CSF). Drug molecules dissolved in CSF escape to the systemic circulation along the CSF drainage routes. One of such routes is through leptomeningeal pores, which have not been sufficiently studied. The goal of this work was to identify approaches to predict the size dependence of the drug clearance from LMS.

We have investigated the process of clearance of macromolecules and particles of various sizes, from ca. 3 nm to 0.6  $\mu$ m, by Positron Emission Tomography (PET). The early data suggest that although the major population of leptomeningeal pores is large ( $>1 \mu$ m), there is apparently another, previously unknown subset of smaller pores. The effective/functional size distributions of the pore populations as well as the anatomical location of the smaller subset are unknown and require further investigation.

## INTRODUCTION

Successful therapy of many disorders involving CNS would benefit from effective delivery of macromolecular or supramolecular drugs to the brain. The intravenous route to CNS is not effective due to the barrier system physically and metabolically preventing the macromolecules from entering CNS tissues from the blood. The leptomeningeal (intrathecal) route provides an alternative approach through CSF, which contacts CNS tissues directly with no barriers between them. However, the fraction of the administered dose delivered to the CNS via this route, and, consequently, the efficacy of the treatment, will depend on the duration of the drug residence in CSF.

According to the current paradigm, CSF is produced by the choroid plexus in brain ventricles and drains into systemic circulation mainly in the arachnoid villi (AV) that are most abundant in the superior sagittal sinus. AV is a web-like structure of interlacing cords, continuing into the dura matter. In the sinus, the cords turn into delicate tissues covered by a layer of mesothelial cells, which separates CSF in the AV lumen from the blood in the sinus.<sup>2</sup> Based on scanning electron microscopy data, a pore-transfer mechanism of CSF passage via mesothelial cells was proposed<sup>3</sup> where the pore size was estimated as being several micrometers.<sup>4</sup>

If CSF is drained through pores (whether static openings or active transcytosis-like processes) the rate of

macromolecule (and nanoparticle) clearance from CSF should depend on both the macromolecule and pore size distribution. The goal of this work was to investigate if PET imaging with radiolabeled macromolecules and particles administered to CSF provides an approach to pore size measurement. Here we report early data suggesting that quantitative PET imaging is an adequate method for investigating the functional size of the leptomeningeal pores.

## EXPERIMENTAL METHODS

Clearance of macromolecules and nanoparticles from LAS of rats and non-human primates was investigated within broader studies of the pharmacokinetics of intrathecally administered proteins, linear polymers and supramolecular constructs (synthetic latexes, phage and virus particles).

PET with <sup>124</sup>I enables short- and long-term (several days) quantitative imaging studies of large molecule/particle pharmacokinetics.<sup>5</sup> All proteins and preparations containing proteins were labeled via direct iodination with iodogen, generally as in our previous studies.<sup>1,5</sup> Model dextrans were first modified with tyrosine (3% of monomer units) to introduce iodination sites. All radiolabeled preparations were treated with metabisulfite and desalted by either gel chromatography on Sephadex G-25 or (polystyrene particles) by centrifugation. Macromolecular preparations were studied by size exclusion HPLC with UV and gamma detection for radiochemical purity ( $>95\%$ ).

The hydrodynamic diameters of the model preparations were determined by size exclusion HPLC using calibration by proteins with known hydrodynamic diameters: thyroglobulin (molecular weight  $M_w=670$  kDa, Stokes radius  $R_s=8.5$  nm),  $\gamma$ -globulin ( $M_w=158$  kDa,  $R_s=5.25$  nm), ovalbumin ( $M_w=44$  kDa,  $R_s=3.05$  nm), myoglobin ( $M_w=17$  kDa,  $R_s=1.9$  nm) and vitamin B<sub>12</sub> ( $M_w=1.35$  kDa,  $R_s=0.84$  nm).

All animal experiments were carried out in accordance with institutionally approved protocols. Normal 150-350 g Sprague-Dawley rats and 1-6 kg cynomolgus monkeys were used as animal models.

The labeled preparations were injected either directly into cisterna magna through the atlanto-occipital junction (rats) or through an intrathecal catheter equipped with a subcutaneous injection port. The amount of <sup>124</sup>I was ca. 0.1 mCi per rat and 0.5 mCi per monkey.

Animals were imaged on either MicroPET P4 (Concord Microsystems/Siemens) or a custom PET/CT system consisting of Siemens microPET Focus 220 and NeuroLogica NL3000 CereTom CT scanners. Dynamic

imaging was carried out for the first 20 minutes after the injection; then whole body scans were acquired at several time points.

The data were reconstructed into the image matrix with fixed slice thickness by iterative OSEM3D/MAP algorithm.

The label content in tissues was measured in manually drawn regions of interest. For each preparation, the data were tabulated; mean values and standard deviations were calculated where applicable.

## RESULTS AND DISCUSSION

The early data obtained with proteins and virus and phage particles showed that a significant fraction (30-50%) of all studied preparations were able to penetrate from LMS to systemic circulation within 3-5 hours and accumulate in the same organs as after intravenous administration. The fact that large virions and phage particles (up to 0.6  $\mu\text{m}$  studied to date) were able to leave LMS suggested that there is a set of large channels acting as pores. However, significant differences in the clearance rates were observed also for much smaller 5-15 nm protein molecules, which suggested that there could be a smaller pore subset.

To exclude the influence of the possible specific macromolecule/particle interactions with cells, further experiments were carried out using fractionated tyrosin-modified dextrans and albumin-coated nanoparticles. After the injection, both polymers were rapidly and uniformly distributed over LMS (excluding lower spine). For the comparative analysis of polymer/particle clearance from CSF, total activity in cranial and spinal compartments at different time points was taken (example in Fig. 1).

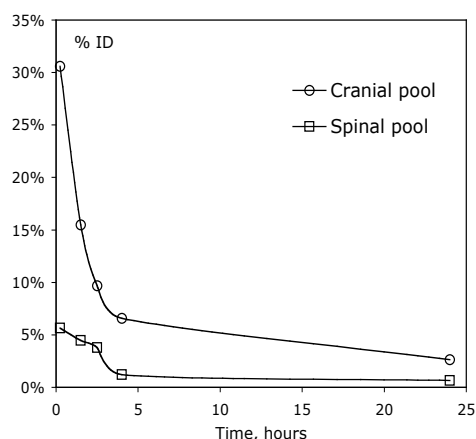


Figure 1. Dynamics of 3.8 nm polymer clearance from LMS, percentage of injected dose (ID) 15 min after injection.

For polymers, in particular, it was estimated that 15 min after injection,  $31 \pm 6\%$  of 3.8 nm polymer and  $42 \pm 10\%$  of 7 nm polymer were in the cranial pool. The dynamics of polymer clearance from CSF were noticeably different (Fig. 2). Within 4 hours after injection, almost 80% of the smaller polymer were transferred to the

systemic circulation, while only 50% of the larger 7 nm polymer were transferred at the same time point. After 24 hours, ca. 10% and 30%, respectively, still remained in LMS. Analogous studies with albumin-coated nanoparticles are currently in progress.

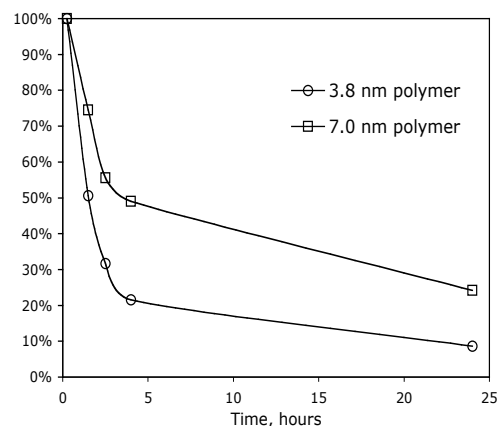


Figure 2. Dynamics of polymers clearance from cranial segment after intrathecal injection in percentage of initial (15 min after injection) uptake.

## CONCLUSION

Clearance of macromolecules and particles from CSF into systemic circulation is size-dependent. The data obtained with particles suggests that there is clearly a set of transport channels functioning as very large pores; the size distribution needs further investigation. However, the size dependence observed for smaller, 3-15 nm molecules, suggests that there may be another subset of pores with smaller effective diameters, which has not been previously described.

The obtained results are relevant to the development of drugs intended for delivery to CNS through leptomeningeal (intrathecal) route. The obtained preliminary data on the pore sizes warrant further investigation.

## REFERENCES

1. Calias P.; Papisov M.; Pan J.; Savioli N.; Belov V. et al. *PLoS ONE* **2012**, 7, (1), e30341-1-13.
2. Weed L.H. *Anat Rec* **1917**, 12, 461-496.
3. Tripathi B.J.; Tripathi R.C. *J Physiol* **1974**, 239, 195-206.
4. Tripathi R.C. *Brain Res* **1974**, 80, 503-506.
5. Belov V.V.; Bonab A.A.; Fischman A.J.; Heartlein M.; Calias P. and Papisov M.I. *Molecular Pharmaceutics* **2011**, 8, (3), 736-747.

## ACKNOWLEDGMENTS

This work was supported by NIH grant R21 CA152384, DoD grant BC100684, and grants from Shire HGT, which also provided model proteins and equipment.

# A PET based method for real time monitoring of drug concentration in the liquid phase of the leptomeningeal compartment

V. Belov<sup>1,2,3</sup> and M. Papisov<sup>1,2,3</sup>

<sup>1</sup>Massachusetts General Hospital, Boston, MA, 02114, USA; <sup>2</sup>Shriners Hospitals for Children, Boston, MA, 02114, USA; Harvard Medical School, Boston, MA, 02115, USA

[vbelov@partners.org](mailto:vbelov@partners.org)

## ABSTRACT SUMMARY

Positron Emission Tomography (PET) is a fully quantitative imaging modality able to accurately measure the concentration of a drug labeled with a positron emitting radionuclide in each part of the body in real time. Quantitative investigation of leptomeningeal (intrathecal) pharmacokinetics by PET is highly instrumental in the development of drugs with complex pharmacokinetics, such as ones intended for delivery to CNS via intrathecal route [1]. Limitations of PET relate to the areas where the drug resides in a liquid compartment and in fibers of tissue penetrating the liquid, as in the leptomeningeal space (LMS). This typically necessitates frequent sampling of the liquid to estimate the share of the solute in the total values measured by PET. The objective of this study was to develop an alternative method utilizing only PET imaging data.

## INTRODUCTION

Drug transport from the intrathecal injection point to CNS tissues in cerebrospinal fluid (CSF) is complex and includes convective processes facilitated by the pulsatile motion of tissues and governed by the geometry of the liquid compartment and other factors. A fraction of the drug can be absorbed by the arachnoid tissues lining and penetrating the liquid compartment. In the PET image, these tissues are not resolved from the liquid compartment. Partial volume effect also complicates the situation, especially in preclinical studies in animals, where the layer of CSF, especially in the spine, is very thin. This necessitates periodic sampling of the liquid to measure drug concentration in it *ex vivo*. The total volume of CSF is not large, and frequent sampling with or without replacement can distort the data. If the sample volume is small, measurements are compromised due to the mixing of the sample with the residual liquid remaining in the port or/and collection catheter from the previous sampling or port flushing.

Considering the importance of resolving the liquid and solid phase components of the leptomeningeal space, we developed a PET based technique for selective investigation of CSF.

In this study, we propose measuring the concentration of the <sup>124</sup>I-labeled compound in CSF by PET in the catheter connecting the injection port and LMS.

In a separate study [2] we investigated the performance and quantification of PET imaging with <sup>124</sup>I and demonstrated its advantages for pharmacological research as well as limitations.

## EXPERIMENTAL METHODS

Cynomolgus macaques with surgically implanted subcutaneous lumbar port (PAS Elite, Smith Medical, MN) were used in the study. The port was connected to the subcutaneous catheter inserted in the LMS. Port served for both drug administration and CSF collection. Model drugs labeled with <sup>124</sup>I were injected by slow bolus through the port, after which the port was flushed with isotonic saline.

Imaging was carried out in accordance with institutionally approved protocols using a custom imaging system consisting of a microPET Focus 220 scanner (Siemens) and CereTom NL 3000 CT scanner (NeuroLogica). The scanners were aligned to ensure reliable PET/CT image registration.

Focus 220 works in 3D mode and features a 22 cm animal opening, axial field of view (FOV) 7.6 cm and transaxial FOV 19 cm. The scanner's detection system provided a 2.1 mm spatial resolution for <sup>124</sup>I. CereTom NL 3000 is a 6-slice tomograph with high-contrast resolution of 0.4 mm (developed for human head imaging in ICU). Animals were sedated and set on a custom extended microPET bed in a supine position, head first, and positioned in the PET imager's field-of-view (FOV). For the duration of the imaging session the animals were given continuous Isofluran/O<sub>2</sub> anesthesia.

The radiolabeled preparations were administered in 1 mL volume slowly over 1 minute, followed by flushing with saline, 0.5 mL/kg body weight. In most studies, the injected amount of <sup>124</sup>I was between 0.5 and 1 mCi (in the example shown below 386  $\mu$ Ci). The duration of PET data acquisition was 5 minutes per single bed position. A whole body CT scan followed the PET. The area of the injection port and catheter was scanned before and after collecting a CSF sample via the port. The list-mode data were reconstructed using OSEM3D/MAP iterative algorithm. The corrections for random coincidences, attenuation and scatter of annihilation photons, detectors dead-time, radioisotope decay as well as normalization to correct for the variation in detector efficiencies and distortion were applied to make the imaging fully quantitative. Attenuation and scatter corrections were based on CT images. Co-registration of the reconstructed PET and CT images was done manually using the tools implemented in the imager's software package. The images of the adjacent bed positions were stitched together using the software tool.

The essence of the method being developed is based on the fact that, although drug concentration inside the catheter can not be measured due to the insufficient resolution, the total amount of radioactivity in a segment of the catheter can be. Thus, for each measurement only a relatively small volume of CSF can be withdrawn to the

catheter (rather than through the catheter and port) for measurement.

Thus, a segment of the catheter of a certain length was selected in the reconstructed image as ROI. The total activity of  $^{124}\text{I}$  in it was determined and divided by the volume of segment to obtain the concentration value. The internal volume of the catheter was measured experimentally. An isolated segment was filled with 10 uL of a contrast agent (Ultravist (Iopromide), 300 mgI/mL) with the aid of Hamilton syringe. The length occupied by liquid was measured in a CT image. The count-rate in the CSF sample withdrawn from the port was measured in a gamma counter (1480 Automatic Gamma Counter, Wallac Wizard 3"). To convert the count-rate into the activity concentration a cross-calibration curve between the gamma counter and the dose calibrator (AtomLab 100, Biodex Medical Systems) was used. PET scanner was calibrated for quantification against the same dose calibrator.

## RESULTS AND DISCUSSION

A PET/CT image of injection port area is shown in Figure 1. CT image demonstrates the port and catheter configuration in the monkey. PET image shows the radiolabeled compound distribution in the CSF and its retention in the port. The total activity remaining in the port after flushing was 0.36 percent of the injected dose (ID). In other animal studies utilizing the same type of port, the maximal residual activity in the port was as high as 5.5% ID. After taking a CSF sample from the port, the total activity in the port increased to 1.91% ID.

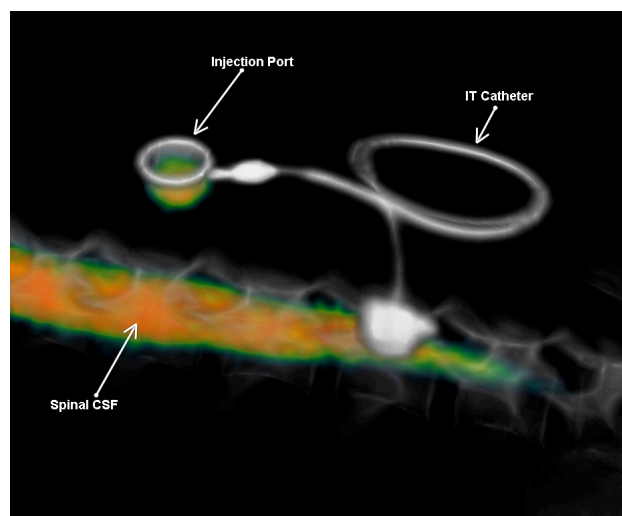


Figure 1. PET/CT image of the lumbar body region of the monkey 30 minutes after administration of the radiolabeled compound with the following flushing.

The catheter connecting the injection port with LMS has a double loop configuration with two straight regions, near the port and near the entrance in the vertebrae. The connection of the catheter with a port has a variable thickness. Another straight region is very close to the spine, where high activity of the spinal CSF may distort

the imaging data. The small portion of the distant curve of the catheter's loop (Figure 2) is most suitable for the measurements. A small region of it (5.572 mm) was taken as ROI in the PET image. The activity in the several analogous ROIs was averaged.

The diameter of catheter was found to be 0.512 mm. In this example, the  $^{124}\text{I}$  concentration in the catheter measured by PET was found to be 46327 nCi/cc vs. sampled CSF that had 31265 nCi/cc as measured ex vivo.

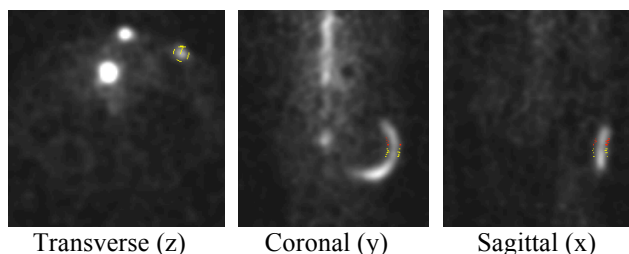


Figure 2. PET images (three projections) of the catheter filled with CSF after withdrawal of a CSF sample. 1.5 hr after injection of an  $^{124}\text{I}$  labeled nanoparticles. ROIs used for activity calculation are shown by yellow and red lines.

The difference is between in-catheter and ex vivo measurements is expected and explained by the dilution of the CSF sample with the liquid remaining in the catheter and port after the previous flushing. Unless a very large volume of CSF is withdrawn from the port before sampling, the result of the measurement is distorted. CSF withdrawal to the catheter, on the other hand, provides undiluted fluid from LMS.

The proposed method requires certain corrections applied to the data during PET image acquisition, which should be taken into account in study planning.

## CONCLUSION

PET imaging enables non-invasive quantification of the concentration of radiolabeled drugs in the liquid compartment of the leptomeningeal space.

## REFERENCES

1. Calias P, Papisov M, Pan J, Savioli N, Belov V, et al. (2012) CNS Penetration of Intrathecal-Lumbar Idursulfase in the Monkey, Dog and Mouse: Implications for Neurological Outcomes of Lysosomal Storage Disorder. PLoS ONE 7(1): e30341. doi:10.1371/journal.pone.0030341.
2. Belov VV, Bonab AA, Fischman AJ, et al. Iodine-124 as a label for pharmacological PET imaging. Molecular Pharmaceutics. 2011; 8(3): 736-747.

## ACKNOWLEDGMENTS

This work was supported by NIH grant R21 CA152384, DoD grant BC100684, and grants from Shire HGT and Neurophage Pharmaceuticals.

# Physiology of intrathecal bolus as revealed by quantitative PET studies

M.I. Papisov,<sup>1-3</sup> V. Belov,<sup>1-3</sup> A.J. Fischman,<sup>3</sup> J. Titus,<sup>1</sup> M. Gagne,<sup>1</sup> C. Gillooly,<sup>1</sup> A. Bonab,<sup>1-3</sup> and D. Levine<sup>1</sup>

<sup>1</sup>Massachusetts General Hospital, Boston, MA; <sup>2</sup>Harvard Medical School, Boston, MA; <sup>3</sup>Shriners Hospitals for Children, Boston, MA.

papisov@helix.mgh.harvard.edu

## ABSTRACT SUMMARY

The overall goal of our studies was to investigate the *in vivo* transport of biopharmaceuticals administered to the cerebrospinal fluid (CSF) and to develop methodology for fully quantitative non-invasive studies of solute dynamics in CSF by Positron Emission Tomography (PET).

Presently, there are no effective treatments to alleviate several conditions involving CNS and meninges, such as neurodegenerative disorders, genetic diseases and cancer. Several recent reports have shown significant biological effects after intrathecal administration of macromolecules and gene vectors. Therefore, a “back door” through the CSF to the CNS may be available for such drugs. However, the intrathecal route to the CNS relies on transport processes that depend on insufficiently studied factors. Using non-invasive quantitative PET imaging, we show how intrathecal bolus can be used for drug delivery to the CNS.

## INTRODUCTION

Intrathecal administration is a clinically viable and frequently used route of drug delivery. Administration of “small-molecule” drugs to the CSF in the distal lumbar area is widely used for pain and spasticity management. These drugs target spinal nerve roots and superficial layers of the spinal cord. The administration is often chronic (months or years), through surgically implanted electronic pumps. The action of such intrathecally administered drugs generally does not extend far beyond the distal spinal sections of CNS where they are administered. However, intrathecal administration of macromolecules and gene vectors have resulted in biologically significant outcomes in the CNS. In view of the high potential value of drug delivery to the brain, it was important to determine what factors can make the delivery of drugs administered to the distal lumbar CSF more efficient than previously believed.

Previous publications suggested the existence of a downdraft of CSF in the spine. Physiologically, such downdraft would depend on CSF drainage at the nerve roots (along with the cerebral drainage through the arachnoid granulations). CSF is produced mostly in the choroid plexus in the brain ventricles; the replacement rate varies in different species, from 0.89% of the total volume per minute in the mouse to 0.38% per minute in man. Considering this high rate of CSF production, a significant spinal CSF drainage could potentially block drug access from the distal spine to the brain “against the flow”.

Drug entrance from the CSF to the CNS parenchyma is another factor to be considered. Even if a significant amount of a drug is delivered to the brain surface, direct diffusion into the brain (even though there is no barrier at the brain surface) against the interstitial outflow would

not enable drug penetration deep into the parenchyma (especially in larger animals and especially for large molecules and nanoparticles).

Investigation of processes occurring in a liquid compartment such as CSF can give distorted results unless non-invasive imaging methods are used for data acquisition. Investigation of complex transfer processes also benefits from methods enabling whole-body quantitative registration of all transfer processes on all time frames and real-time data acquisition in the same animal, which excludes the individual variances from the kinetic data. PET, as a powerful tool for quantitative *in vivo* imaging of the transport of pharmaceuticals labeled with positron-emitting radionuclides, meets the above requirements. Therefore, we used PET to investigate the transport of intrathecally administered macromolecules and particles. Non-human primates were used as a model phylogenetically close to humans.

## EXPERIMENTAL METHODS

Four human recombinant enzymes (iduronate-2-sulfatase (I2S), arylsulfatase A (ARSA), heparan-N-sulfatase (HNS), galactosylceramidase (GALC), particles of phage M13, model macromolecules (poly[hydroxymethylethylene hydroxymethylformal]) and amorphous silica nanoparticles were labeled with <sup>124</sup>I and administered at various doses via intrathecal routes (cisterna magna, distal lumbar segment, cerebral ventricle).

Among positron emitters available and suitable for PET, <sup>124</sup>I has the longest physical half-life of 4.2 days. This, combined with the well-investigated iodine behavior *in vivo*, makes <sup>124</sup>I attractive for long-term (several days) imaging studies. We have shown in our previous studies <sup>124</sup>I provides fully quantitative data suitable for pharmacological research. Some experiments were carried out using <sup>89</sup>Zr. While the physical half-life of this radionuclide is shorter than of <sup>124</sup>I, the behavior of <sup>89</sup>Zr *in vivo* after the degradation of the labeled material is different that of iodine. While the latter, in the form of iodide, leaves the cells where the labeled material is degraded, <sup>89</sup>Zr remains in the cells, providing images unaffected by catabolism.

Imaging was carried out using a custom PET/CT imaging system consisting of MicroPET Focus 220 PET scanner (Siemens, DC) and CereTom CT scanner (Neurologica, MA).

The general scheme of the non-human primate experiments is shown in Figure 1. The labeled substances were administered through a subcutaneous port connected through a subcutaneous catheter with the leptomeningeal space in the lower lumbar area or in the cerebral ventricles. In rats, intrathecal administration was carried out either via direct injection to cisterna magna through the Atlanto-Occipital joint, or through a surgically installed lumbar or cisternal catheter.

Dynamic imaging data (0-20 min post injection) and multiple static images were acquired over up to 8 days after the injections. Acquisition, histogramming, and reconstruction were executed using Siemens software. CT images were used for attenuation correction and (as in Figure 1) for anatomical referencing. The numerical data from manually selected regions of interest were processed to determine the principal PK parameters.

Fluorophore-labeled macromolecules were utilized to investigate by photoimaging the microdistribution of the administered substance.

## RESULTS AND DISCUSSION

For all agents, the initial distribution of the administered substance was found to depend on the administered volume (administration of volumes up to 30% of the total estimated CSF volume is safe for primates, both human and non-human).

We have found that a low-volume (< 0.5 ml) lumbar intrathecal injection forms a pool in the CSF that slowly extends in both directions from the injection point (not shown), whereas the same substance administered in a larger volume is immediately delivered to the cerebral CSF (Figure 1). Only a small fraction of the injected volume moves distally from the injection point.

Solute clearance from the spinal CSF was found to be size dependent. While all larger macromolecules (hydrodynamic diameter > 7 nm) were cleared with the half-life of 4-5 hours (rats and monkeys), which is consistent with the rate of CSF exchange, for smaller macromolecules (3.7 nm) the clearance half-life was ca. 2 hours (rat). For both D- and L- glucose the initial clearance half-life was 15 min (45% of the administered fraction).

A large volume delivered to the ventricle spreads in the cerebral CSF and in the neck area, but does not enter the spine. This suggests that the hydrostatic compliance of the compartment is centered in the cerebral area and relates, most likely, to the compliance of the large cerebral veins and, possibly, a somewhat flexible section of dura in the neck.

Images of all animals that received enzyme injections (monkeys, n=28, rats, n=36) were studied for signs of lymphatic accumulation (that would mark CSF drainage through nerve roots or blood vessels). Only in animals with leakages at the injection point (needle injection) the sentinel lymph nodes draining the injection site were radioactive. In catheterized animals, minor sentinel node labeling was observed in the catheter insertion area only in one monkey and three rats.

For all administered enzymes, macromolecule penetration from the CSF into the brain was quantified from the imaging data. In *M. Fascicularis* at 2.5 hours after the injection up to ca. 10-15% of the intrathecally administered dose of proteins and phage particles can be localized in the brain volume (excluding the ventricles), and by 24 hours this value decreases to 1.5-2% of the injected dose, in some animals up to 6%. The subsequent washout is slower (estimated half-life 15-20 hours). This is in agreement with the entrance of the solute from CSF to the perivascular space during the first hours after the injection, when the solute concentration in the CSF is still high, followed by partial exit of the solute back to the CSF when its concentration in the latter is significantly reduced due to the CSF replacement (drainage). The remaining fraction is most likely transferred from the perivascular space to the parenchyma and taken up by the CNS cells, and the slower subsequent process of the label

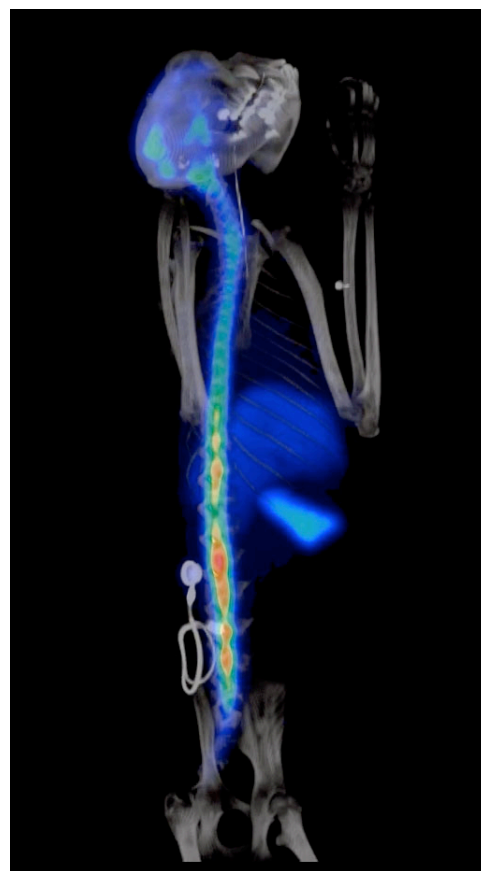


**Figure 1.** Scheme of the non-human primate experiment (PET/CT projection image).

Proteins were administered through a subcutaneous port connected through a subcutaneous catheter with the leptomeningeal space.

Color represents 3-dimensional quantitative map of the protein concentration as measured by PET (shown: 5 hours after the injection).

washout relates to the deiodination of the administered material. Photoimaging studies indicated enzyme deposition in pia mater as well as deep in the brain parenchyma (both grey and white matter).

## CONCLUSIONS

The efficacy of the intrathecal CNS targeting depends on the physiology of the intrathecal bolus, which is sensitive to the administered volume. There is no downdraft of CSF in the spine that would prevent drug access to the cranial CSF.

The high rates of both solute spread in the CSF and entrance to the CNS parenchyma can not be explained by diffusion and rely on active transport processes, most likely pulsation-assisted convection in the subarachnoid and perivascular spaces.

Solute clearance from the CSF is size-dependent and relies not only on the large (micron-range) pores found in the arachnoid granulations.

## ACKNOWLEDGEMENTS

This work was supported by NIH R21 CA152384, DoD BC100684, and grants from Shire HGT and Neurophage Pharmaceuticals.

## Dynamics and solute transport in CSF in non-human primates as seen by Positron Emission Tomography

Mikhail I. Papisov

Massachusetts General Hospital, Harvard Medical School and Shriners Hospitals for Children.

**Abstract.** The overall goal of our studies was to investigate the in vivo transport of enzyme replacement therapeutics and other macromolecules and particles administered to the CSF. In particular, the studies were intended to evaluate the role of CSF flows in the drug transport from the cerebroventricular and lumbar CSF sub-compartments. The studies were also intended to evaluate the relevance of rodent models, as compared with primate models, and to develop methodology for fully quantitative non-invasive studies of solute dynamics in CSF by Positron Emission Tomography (PET).

Presently, there are no effective treatments to alleviate several conditions involving CNS, such as neurodegenerative disorders, genetic diseases and cancer. With the growing number of biopharmaceuticals and drug-carrying nanoconstructs entering preclinical and clinical studies, quantitative investigation of their behavior in vivo is playing an increasingly important role in view of the well-known problems with the large molecule and particle transport through tissue barriers, especially the blood-brain barrier. Several recent reports have shown significant biological effects of the intrathecal administration of macromolecules and gene vectors. Therefore, a “back door” through the CSF to the CNS may be available for such drugs. However, the intrathecal route to the CNS relies on processes that depend on insufficiently studied factors, such as remixing of CSF by the pulsatile movement of the CNS tissues, drainage of CSF to the blood through mesothelial pores, and intraparenchymal interstitial and non-interstitial transfer. Several contradictory conclusions have been made regarding the role of the CSF dynamics in the outcome of the process. Investigation of complex combinations of transfer processes benefits from methods enabling: (i) whole-body quantitative registration of all transfer processes on all time frames, and (ii) real-time data acquisition in the same animal and using any animal as its own control, which removes the individual variances from the kinetic data. PET, as a powerful tool for quantitative in-vivo imaging of the transport of pharmaceuticals labeled with positron-emitting radionuclides, meets the above requirements. The studies were carried out using  $^{124}\text{I}$  as a radiolabel; among all currently available positron emitters suitable for PET,  $^{124}\text{I}$  has the longest physical half-life (4.2 d) and a well established catabolism.

The results of the studies have demonstrated that CSF dynamics (i) is the major factor of the initial distribution of the administered solute in the CSF compartment, and (ii) plays a significant role in the subsequent solute redistribution concurrent with entrance to the CNS and drainage to the systemic circulation. Rodent model was shown to be relevant and potentially scalable.

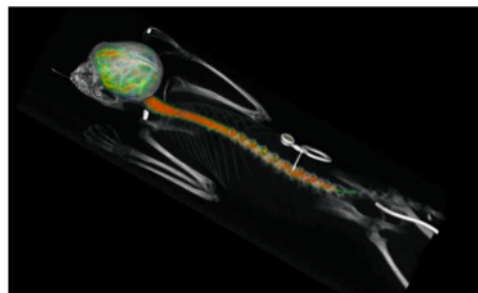


**Figure 1.** Scheme of the non-human primate experiment (PET/CT image). Radiolabeled proteins and particles were administered through a subcutaneous port (center) connected through a subcutaneous catheter with the leptomeningeal space. Color represents 3-dimensional map of the protein concentration as measured by PET (shown: 3 hours after the injection).



**About the Presenter.** Mikhail (“Misha”) Papisov, PhD, Associate Chemist (Massachusetts General Hospital), Assistant Professor of Radiology (Harvard Medical School). Head of Molecular Pharmacology and Pharmacological Imaging laboratory. Received his M.S. in Chemistry from Moscow State University in 1982 and Ph.D. in Biology from the National Cardiology Research Center of the Academy of Medical Sciences in Moscow in 1988. Research focus: development of macromolecular and nano-therapeutics with emphasis on novel physiological aspects of macromolecule transport in vivo, structure-function relationships and quantitative preclinical PET imaging; PET studies of macromolecule and particle transport in the CSF.